Accepted Manuscript

An innovative modal approach for frequency domain stress recovery and fatigue damage evaluation

Claudio Braccesi, Filippo Cianetti, Lorenzo Tomassini

PII: S0142-1123(16)00077-3
DOI: http://dx.doi.org/10.1016/j.ijfatigue.2016.02.028
Reference: JIJF 3865

To appear in: *International Journal of Fatigue*

Received Date: 2 July 2015
Revised Date: 16 February 2016
Accepted Date: 19 February 2016

Please cite this article as: Braccesi, C., Cianetti, F., Tomassini, L., An innovative modal approach for frequency domain stress recovery and fatigue damage evaluation, *International Journal of Fatigue* (2016), doi: http://dx.doi.org/10.1016/j.ijfatigue.2016.02.028

An innovative modal approach for frequency domain stress recovery and fatigue damage evaluation

Claudio Braccesi, Filippo Cianetti*, Lorenzo Tomassini

University of Perugia, Department of Engineering, via G. Duranti, 93, Perugia, 06125 Italy

Abstract

The aim of the present paper is to show and validate an innovative method, developed by authors to evaluate, in frequency domain, the fatigue damage of mechanical components modeled by modal approach and subjected to random dynamic loads. The authors, in particular, have theoretically demonstrated that the exact statistical properties (*spectral moments*) of the PSD functions matrix of stress tensor of the model are obtainable only from PSD functions matrix of its modal coordinates and from PSD functions matrix of inputs. To show the capabilities of this new approach and to verify the obtainable speeding up of the evaluation process two test cases are analyzed and discussed.

Keywords: random loads; frequency domain analysis; modal approach; vibration fatigue; spectral moments

1. Introduction

The evolution, in last three decades, of the techniques of analysis and evaluation of fatigue damage in frequency domain of components subjected to random loads has brought this kind of approach to be an established feature in the scenario of fatigue design.

Even if the attention was addressed only to fatigue damage evaluation, starting from works of Whirsching [1] or Bendat [2], it is possible to notice a great progress in the approaches developed to evaluate load spectra or fatigue damage directly from the frequency domain representation of the components of stress state tensor, developed from theoretical, numerical or experimental point of view [3-24].

Whatever consolidated criteria is considered, it assumes to have a single stress power spectral density (PSD) function [2, 25-26] as input (i.e. uniaxial stress state). To extend the capabilities of this kind of approach to multiaxial stress states, a lot of criteria were developed to adapt results and methods, designed for uniaxial stress conditions, to multiaxial ones, obtaining encouraging results [27-37].

Starting from a single stress PSD function, so called *direct* [3,8-10,13,22], *correction coefficients* [1,7,11-12,14], and *indirect* [21] criteria allow to obtain an evaluation of the load spectrum and of the cycles *probability density function* (pdf) or to, directly, assess the damage, by adopting a damage cumulation rule, such as the linear *Palmgren-Miner* one [38].

The aim of the present paper is to show and validate an innovative method, developed by authors to evaluate, in frequency domain, the fatigue damage of mechanical components modeled by modal approach and subjected to random dynamic loads.

In previous papers, the authors have focused their attention on the numerical evaluation of the stress state and of the associated fatigue damage of mechanical components subjected to random dynamic loads; this activity was developed starting from the hypotheses of mechanical systems modeled within a multibody code (MBS) and of component/s modeled by using modal approach [16-18, 39-40]. From these hypotheses, the analysis of the dynamic behavior of the component, when performed in the frequency domain, was assumed to have the system representation expressed in a linearized form, as a state space system [2,25], having as inputs whatever loading condition and as outputs the modal coordinates of the component. The latter were associated with the corresponding mode shapes (i.e. stress mode shapes), previously obtained in the component mode synthesis process, carried out in any finite element analysis (FEA) environment. This utility is now implemented in all the major MBS codes, also

* Corresponding author: Filippo Cianetti
E-mail: filippo.cianetti@unipg.it
Phone: +39 075 5853728
Fax: +39 075 5853703

thanks to the research activity of the authors themselves [16,39]. This hypothesis, apparently restrictive, allows to tackle the analysis of non-linear system too, in case of random load conditions [16], by always considering the linear behavior of the component (modal approach). In a previous work the authors have shown that it is possible to successfully deal with these conditions and, therefore, to well recover the matrix of power spectral density functions (PSDs) [16] of the stress tensor of a generic element of the FEA model, by combining time domain dynamic analysis with the previously cited one.

The *reference* frequency domain procedure to evaluate damage was and is a method that, by looping among all elements, reconstructs the power spectral density matrix of the stress tensor, a matrix 6×6, and then summarizes its content in a single power spectral density function [39,4,26,29-31], for example by using *Preumont*'s approach, that can be subjected to any frequency criterion. When the stress state satisfies the hypothesis of Gaussian stationary ergodic signal and is synthesized by a single signal, the literature shows a whole series of approaches that, starting from its power spectral density function (PSD) and the relative *spectral moments*, allow to directly obtain an estimation of the damage [3-24]. *Dirlik*'s one [3] is considered by authors as reference criterion, which, if compared to the other ones, shows a greater applicability to a wide range of PSDs [11-12,23]. A lot of approaches then try to adapt results and methods developed for uniaxial stress conditions to multiaxial stress states with encouraging results [27-31,33,35,36-37].

One of the aims that the research on fatigue arises is to provide the designer with tools that are able to understand the physical behavior of the phenomenon correctly without huge computational costs. The frequency domain stress state recovery (dynamic analysis step) and the use of the above approaches (results post-processing step) allow to reach this aim, especially if their use is oriented to the first stage of the mechanical system design process and, in particular, to the identification of components critical locations.

In order to speed up as much as possible the frequency domain method, the authors have undertaken a further research activity aimed to minimize calculation time and errors in the damage evaluation of flexible components by FEA or multibody (MBS/Flex) approach[39, 18].

This paper demonstrates the capabilities of an innovative stress recovery and statistical content evaluation, especially for finite element analysis calculation environments (FEA). First of all the authors briefly describe the state of the art of performing dynamic numerical analysis in frequency domain. By addressing and illustrating the theoretical problems in using the modal approach, focusing on finite element analysis, a new dynamic simulation procedure, adoptable and easily implementable by FEA codes, is shown. The authors show the theoretical demonstration - of how the fatigue damage of all or of a subset of elements of the model can be assessed with great speed and without error from the knowledge of a set of halfway results of the classical dynamic analysis, without necessarily to recover the *power spectral density* function matrix (PSD) of the stress tensor of each element. The paper- theoretically demonstrates as the statistical properties (*spectral moments* [2,25-26]) of the PSD matrix of the modal coordinates of the model, together with the stress mode shapes, are necessary and sufficient to achieve the statistical properties of the stress tensor PSD functions, and thus to allow, for all the so called "direct" approaches (based on the spectral moments of the stress PSD function), to assess the damage with no margin for error.

Two numerical test cases are presented to show the capabilities of this new approach. For every example a FE shell model of the structure, loaded by single point base motion, is considered. The dynamic analysis was conducted in frequency domain by classical modal approach and, for each element, starting from the PSD function of the equivalent stress (*Preumont*'s approach), the damage was obtained by a frequency domain criterion (*Dirlik*'s one). *Dirlik*'s damage was considered the *reference* damage value for the frequency approach. Previous results are compared with those obtained with the developed and proposed procedure, with the aim to show its goodness (zero error if compared with frequency domain reference results) and how much faster it is (two hundred times faster than the frequency domain reference approach). Two frequency domain criteria were adopted: *Dirlik*'s one and *Bands method*, a criterion proposed by authors in a previous paper [22].

2. Dynamic modelling and simulation

If a generic component and its FEA model, characterized by n degrees of freedom (*dofs*), is considered, the equation of motion is, in general, expressed by the following:

$$\boldsymbol{M}\cdot\ddot{\boldsymbol{\delta}}+\boldsymbol{C}\cdot\dot{\boldsymbol{\delta}}+\boldsymbol{K}\cdot\boldsymbol{\delta}=\boldsymbol{f} \tag{1}$$

where $\boldsymbol{M}$ is the mass matrix $(n\times n)$, $\boldsymbol{C}$ is the damping matrix $(n\times n)$, $\boldsymbol{K}$ is the stiffness matrix $(n\times n)$, $\boldsymbol{f}$ is the vector of forces $(n\times 1)$ and $\boldsymbol{\delta}$ is the displacement vector $(n\times 1)$.

It's possible to rewrite equation (1) by rearranging the degrees of freedom, and consequently vectors $\boldsymbol{\delta}$ and $\boldsymbol{f}$ and the $\boldsymbol{M}$, $\boldsymbol{K}$ and $\boldsymbol{C}$ matrices, by separating the r constrained (boundary) degrees of freedom, denoted by the subscript B, and the s free (internal) degrees of freedom, denoted by the subscript L, as described in (2).

$$\begin{bmatrix}\boldsymbol{M}_{LL} & \boldsymbol{M}_{LB}\\ \boldsymbol{M}_{BL} & \boldsymbol{M}_{BB}\end{bmatrix}\cdot\begin{Bmatrix}\ddot{\boldsymbol{\delta}}_L\\ \ddot{\boldsymbol{\delta}}_B\end{Bmatrix}+\begin{bmatrix}\boldsymbol{C}_{LL} & \boldsymbol{C}_{LB}\\ \boldsymbol{C}_{BL} & \boldsymbol{C}_{BB}\end{bmatrix}\cdot\begin{Bmatrix}\dot{\boldsymbol{\delta}}_L\\ \dot{\boldsymbol{\delta}}_B\end{Bmatrix}+\begin{bmatrix}\boldsymbol{K}_{LL} & \boldsymbol{K}_{LB}\\ \boldsymbol{K}_{BL} & \boldsymbol{K}_{BB}\end{bmatrix}\cdot\begin{Bmatrix}\boldsymbol{\delta}_L\\ \boldsymbol{\delta}_B\end{Bmatrix}=\begin{Bmatrix}\boldsymbol{f}_L\\ \boldsymbol{f}_B\end{Bmatrix} \tag{2}$$

If the dynamic analysis is carried out by adopting a modal representation of the system [26] the displacements of the internal *dofs* L are obtainable by the evaluation of the modal coordinates $\boldsymbol{q}$**,** which are the unknowns of the reduced modal system. This change of coordinates is described by the following relations for the internal or free degrees of freedom:

$$\boldsymbol{\delta}_L(t)=\boldsymbol{\Phi}\cdot\boldsymbol{q}(t) \tag{3}$$

$$\boldsymbol{\delta}_L(t)=\boldsymbol{\Phi}_{\mathrm{C}}\cdot\boldsymbol{\delta}_B(t)+\boldsymbol{\Phi}\cdot\boldsymbol{q}(t) \tag{4}$$

The equation (3) refers to forced vibration instead equation (4) to motion base condition.

In this relations $\boldsymbol{\delta}_L(t)$ represents the physical displacement of the internal or free degrees of freedom of the model at time t $(s\times 1)$, $\boldsymbol{\Phi}$ is a transformation matrix named *modal* $(s\times m)$ with m the number of modes, generally less than or equal to s. $\boldsymbol{q}(t)$ represents the set of coordinates defined by the transformation (*modal coordinates* or *Lagrangian coordinates*) of size $(m\times 1)$. The matrix $\boldsymbol{\Phi}_{\mathrm{C}}$. is a $(s\times r)$ matrix named *constraint modes* [41] and it is equal to the product $-(\boldsymbol{K}_{LL})^{-1}\boldsymbol{K}_{LB}$. Each $\boldsymbol{\Phi}_{\mathrm{C}}$ column represents the deformed shape of L *dofs* when an unitary displacement at the j-th B *dof* is imposed and the other B degrees of freedom are constrained (zero displacement/rotation).

For loading condition characterized by force inputs and by modal transformation the previous time domain motion equations (2) become eqn. (5):

$$\begin{bmatrix}\ddots & & \\ & 1 & \\ & & \ddots\end{bmatrix}\begin{Bmatrix}\ddot{\boldsymbol{q}}\end{Bmatrix}+\begin{bmatrix}\ddots & & \\ & 2\xi\omega_n & \\ & & \ddots\end{bmatrix}\begin{Bmatrix}\dot{\boldsymbol{q}}\end{Bmatrix}+\begin{bmatrix}\ddots & & \\ & \omega_n^2 & \\ & & \ddots\end{bmatrix}\begin{Bmatrix}\boldsymbol{q}\end{Bmatrix}=\boldsymbol{\Phi}^T\boldsymbol{f}_L \tag{5}$$

where the $\boldsymbol{\Phi}^T\boldsymbol{f}_L$ term has dimension $(m\times 1)$.

Instead, for loading condition characterized by motion inputs the motion equations become eqn. (6).

$$\begin{bmatrix}\ddots & & \\ & 1 & \\ & & \ddots\end{bmatrix}\begin{Bmatrix}\ddot{\boldsymbol{q}}\end{Bmatrix}+\begin{bmatrix}\ddots & & \\ & 2\xi\omega_n & \\ & & \ddots\end{bmatrix}\begin{Bmatrix}\dot{\boldsymbol{q}}\end{Bmatrix}+\begin{bmatrix}\ddots & & \\ & \omega_n^2 & \\ & & \ddots\end{bmatrix}\begin{Bmatrix}\boldsymbol{q}\end{Bmatrix}=-\boldsymbol{\Phi}^{\boldsymbol{T}}(\mathbf{M}_{\mathrm{LB}}+\mathbf{M}_{\mathrm{LL}}\boldsymbol{\Phi}_{\mathrm{C}})\,\ddot{\boldsymbol{\delta}}_B \tag{6}$$

The $-\boldsymbol{\Phi}^{\boldsymbol{T}}(\mathbf{M}_{\mathrm{LB}}+\mathbf{M}_{\mathrm{LL}}\boldsymbol{\Phi}_{\mathrm{C}})$ matrix is named *modal participation factors matrix* and it is denoted by γ.

To translate the problem into frequency domain, it is convenient to calculate the frequency response between the m *Lagrangian coordinates* of the model (outputs) and the z inputs, that is the matrix of complex functions $\boldsymbol{H}_q(\omega)$. This matrix, for the generic frequency ω, assumes the dimensions $(m\times z)$. The FRF matrix in terms of stress is obtainable as a linear combination between $\boldsymbol{H}_q(\omega)$ and the stress mode shapes.

The $\boldsymbol{H}_q$ matrix is evaluable by the following equation:

$$\boldsymbol{H}_q(\omega) = \boldsymbol{H}_n(\omega) \cdot \boldsymbol{A} \tag{7}$$

where the term $\boldsymbol{H}_n$ is a (m, m) matrix defined by the following:

$$\boldsymbol{H}_n(\omega) = \begin{bmatrix} \ddots & & \\ & \dfrac{1}{\omega_n^2 + 2\, j\, \xi\, \omega_n\, \omega - \omega^2} & \\ & & \ddots \end{bmatrix} \tag{8}$$

that is the frequency response function of a *sdof* (single degree of freedom) system of unitary mass, ω_n natural frequency and ξ damping ratio.

The matrix $\boldsymbol{A}$ $(m \times z)$ assumes a formulation (i.e. motion inputs) and dimensions (i.e. z) that depend from the inputs type. In the case of force excitation is represented by the following:

$$\boldsymbol{A} = \boldsymbol{\Phi}^{\boldsymbol{T}} \tag{9}$$

for imposed motion condition by the following:

$$\boldsymbol{A} = \boldsymbol{\gamma} \tag{10}$$

If equations (3) and (4) are true for the displacement the same approach is true for the stress recovery of a single element in time domain, if the mode shapes of the same are expressed in terms of stress.

The equations (3) and (4) become the following ones:

$$\boldsymbol{\sigma}(t) = \boldsymbol{\Phi}^{\sigma} \cdot \boldsymbol{q}(t) \tag{11}$$

$$\boldsymbol{\sigma}(t) = \boldsymbol{\Phi}_C^{\sigma} \cdot \boldsymbol{\delta}_B + \boldsymbol{\Phi}^{\sigma} \cdot \boldsymbol{q}(t) \tag{12}$$

where $\boldsymbol{\sigma}$ is the stress tensor at t instant (6×1), $\boldsymbol{\Phi}_C^{\sigma}$ is the *stress constraint modes* matrix $(6 \times r)$ and $\boldsymbol{\Phi}^{\sigma}$ is the *stress modal shapes* one $(6 \times m)$.

To translate the time domain equations (11) and (12) into the frequency domain, *Fourier Transform* operator (FT) [5, 7] must be adopted:

$$\boldsymbol{Q} = \boldsymbol{H}_q F(\ddot{\boldsymbol{\delta}}_B) \tag{13a}$$

$$F(\boldsymbol{\sigma}) = \boldsymbol{\Phi}_C^{\sigma} F(\boldsymbol{\delta}_B) + \boldsymbol{\Phi}^{\sigma} \boldsymbol{Q} \tag{13b}$$

in which $F(\boldsymbol{\sigma})$ is the FT of stress tensor, $\boldsymbol{Q}$ is the FT of modal coordinates, that is a matrix of dimensions $(m \times z)$. The symbol $F(\cdot)$ represent FT operator. $F(\ddot{\boldsymbol{\delta}}_B)$ is the FT of constraints acceleration, a matrix of dimensions $(z \times z)$. $F(\boldsymbol{\delta}_B)$ is the FT of constraints displacement, a matrix of dimensions $(r \times z)$ and $F(\boldsymbol{\sigma})$ is the FT of stress tensor, a matrix of dimensions $(6 \times z)$. By definition [5, 7], at each frequency, the stress PSD matrix $\boldsymbol{G}_\sigma$ (6×6) can be obtained by the following:

$$\boldsymbol{G}_\sigma = F(\boldsymbol{\sigma}) \cdot \bar{F}(\boldsymbol{\sigma})^T \tag{14}$$

where $(\bar{\cdot})$ is the *complex conjugate* operator.

The (14) can be rewritten by using the (13):

$$\boldsymbol{G}_\sigma = F(\boldsymbol{\sigma}) \cdot \bar{F}(\boldsymbol{\sigma})^T = (\boldsymbol{\Phi}_C^{\sigma} F(\boldsymbol{\delta}_B) + \boldsymbol{\Phi}^{\sigma} \boldsymbol{Q}) \cdot (\boldsymbol{\Phi}_C^{\sigma} \bar{F}(\boldsymbol{\delta}_B) + \boldsymbol{\Phi}^{\sigma} \bar{\boldsymbol{Q}})^{\mathrm{T}} \tag{15}$$

Recalling that $F(\boldsymbol{\delta}_B) = -F(\ddot{\boldsymbol{\delta}}_B)/\omega^2$, the (15) becomes:

$$\boldsymbol{G}_\sigma = \boldsymbol{\Phi}^\sigma \cdot \boldsymbol{G}_q \cdot (\boldsymbol{\Phi}^\sigma)^\mathrm{T} + \boldsymbol{\Phi}_\mathrm{C}^\sigma \cdot \frac{\boldsymbol{G}_x}{\omega^4} \cdot (\boldsymbol{\Phi}_\mathrm{C}^\sigma)^\mathrm{T} - \boldsymbol{\Phi}^\sigma \cdot \boldsymbol{H}_q \cdot \frac{\boldsymbol{G}_x}{\omega^2} \cdot (\boldsymbol{\Phi}_\mathrm{C}^\sigma)^\mathrm{T} - \boldsymbol{\Phi}_\mathrm{C}^\sigma \cdot \frac{\boldsymbol{G}_x}{\omega^2} \cdot \left(\overline{\boldsymbol{H}}_q\right)^\mathrm{T} \cdot (\boldsymbol{\Phi}^\sigma)^\mathrm{T} \tag{16}$$

in which the PSD matrices of inputs $\boldsymbol{G}_x$ $(z \times z)$ and of modal coordinates $\boldsymbol{G}_q$ $(m \times m)$ are defined by the following equations. For acceleration inputs condition $z = r$.

$$\boldsymbol{G}_x = F\left(\ddot{\boldsymbol{\delta}}_B\right) \cdot \bar{F}\left(\ddot{\boldsymbol{\delta}}_B\right)^T \tag{17a}$$

$$\boldsymbol{G}_q = \boldsymbol{Q} \cdot \overline{\boldsymbol{Q}}^T = \boldsymbol{H}_q \cdot \boldsymbol{G}_x \cdot \boldsymbol{H}_q^T \tag{17b}$$

Equation (16) could be used to analyze force inputs condition too, by simply neglecting the static contribution to the stress state and considering only its first term:

$$\boldsymbol{G}_\sigma = \boldsymbol{\Phi}^\sigma \cdot \boldsymbol{G}_q \cdot (\boldsymbol{\Phi}^\sigma)^\mathrm{T} \tag{18}$$

where $\boldsymbol{G}_q$ is calculated by the (17b), $\boldsymbol{H}_q$ is defined by (7), (8) and $\boldsymbol{G}_x$ by the following:

$$\boldsymbol{G}_x = F(\boldsymbol{f}_L) \cdot \bar{F}(\boldsymbol{f}_L)^T \tag{19}$$

with $F(\boldsymbol{f}_L)$ the FT of forces vector $(s \times 1)$. For load inputs condition $\boldsymbol{G}_x$ has dimensions $(z \times z)$ with $z = s$.
Usually only few internal *dofs* are loaded and z is less than s.
The result of this first part of the paper is the proposal to implement in FEA codes a dynamic analysis procedure for the evaluation of the stress state by PSD frequency analysis which identifies the following steps and obtains halfway results, directly accessible by the user:

- definition of the PSD matrix $\boldsymbol{G}_x$ of the inputs,
- constrained modal analysis aimed at obtaining the natural frequencies ω_n of the system and the stress modal matrix $\boldsymbol{\Phi}^\sigma$ and of any other output is desired as the output of an element subset or of all elements,
- static analyses with imposed unitary displacement for the evaluation of the stress matrix $\boldsymbol{\Phi}_\mathrm{C}^\sigma$ (analyses needed for accelerations input) and of any other output is desired as the output of an element subset or of all elements,
- evaluation of the FRF matrix of modal coordinates $\boldsymbol{H}_q$,
- evaluation of the PSD matrix of modal coordinates $\boldsymbol{G}_q$.

These results could be post or directly processed into the FEA code, by means of relation (16) and/or (18), or accessible by the user as an halfway result and exportable for FC codes, in which it might be useful to implement these relations. If compared with the heavy computational effort of the fatigue codes, this approach would avoid the FEA code to evaluate an high number of frequency response functions matrices, expressed in terms of stress $\boldsymbol{H}_\sigma$ with dimensions $(6 \times z)$, equal to the number of the elements. It only needs the calculation of a single matrix $\boldsymbol{H}_q$ $(m \times z)$, and allows to obtain stress PSD matrix $\boldsymbol{G}_\sigma$ (6×6) of the elements through trivial matrix products, when the terms showed into the previously steps are known.

The result of a generic FE frequency domain dynamic analysis will be, for the generic *j*-th element (of a finite elements model), a matrix (6×6) $\boldsymbol{G}_\sigma$ of power spectral density functions, representative of a general multiaxial stress state [39]. the relations, respectively for forced vibration and motion base conditions, to obtain $\boldsymbol{G}_\sigma$ are the following:

$$\boldsymbol{G}_\sigma = \boldsymbol{\Phi}^\sigma \cdot \boldsymbol{G}_q \cdot (\boldsymbol{\Phi}^\sigma)^\mathrm{T} \tag{18}$$

$$\boldsymbol{G}_\sigma = \boldsymbol{\Phi}^\sigma \cdot \boldsymbol{G}_q \cdot (\boldsymbol{\Phi}^\sigma)^\mathrm{T} + \boldsymbol{\Phi}_\mathrm{C}^\sigma \cdot \frac{\boldsymbol{G}_x}{\omega^4} \cdot (\boldsymbol{\Phi}_\mathrm{C}^\sigma)^\mathrm{T} - \boldsymbol{\Phi}^\sigma \cdot \boldsymbol{H}_q \cdot \frac{\boldsymbol{G}_x}{\omega^2} \cdot (\boldsymbol{\Phi}_\mathrm{C}^\sigma)^\mathrm{T} - \boldsymbol{\Phi}_\mathrm{C}^\sigma \cdot \frac{\boldsymbol{G}_x}{\omega^2} \cdot \left(\overline{\boldsymbol{H}}_q\right)^\mathrm{T} \cdot (\boldsymbol{\Phi}^\sigma)^\mathrm{T} \tag{16}$$

This matrix $\boldsymbol{G}_\sigma$ is represented in equation (20) and contains the auto-spectra of each of the six components of the stress tensor (21) in the main diagonal and the relative cross-spectra in terms outside of it. This is true whatever dynamic analysis is performed and whatever inputs type is considered.

Obtaining a PSD stress tensor such as that shown in (20) highlights a fundamental problem:

- how to utilise a tensor such as the matrix $\boldsymbol{G}_\sigma(\omega)$ that, in general, in addition to the auto-correlation terms, presents terms of cross-correlation between the stress tensor's components, in the consolidated frequency domain evaluation criteria for fatigue damage, which limit is to consider a single stress random process?

Currently, this result is managed, or directly by the FEA codes or by those developed for the evaluation of the fatigue behaviour (FC), providing the user the possibility to post-process, according to the criteria mentioned before, a single function of the matrix (20), a particular combination of the components of this (i.e. by applying *von Mises*' rule), the PSD function of one of the three stress principal components.

The answer to the above question is of particular interest especially analysing both the theoretical [26-27] and experimental [28] results obtained by several researchers. These results demonstrate that the cross-correlation terms of the PSD stress matrix $\boldsymbol{G}_\sigma(\omega)$ have a strong impact on the calculated fatigue life.

According *Lagoda* and *Macha* [27], all of the 36 PSD functions of the matrix (20) should be appropriately considered, without neglecting the terms outside the main diagonal [39]. To this end, as shown in papers [16,35,39], the approach proposed by *Preumont* [4,26,29-31] (*equivalent von Mises stress*, EQVM) could be considered an useful procedure to synthesize into a single PSD function the full stress state. Moreover, it could be easily implemented in any FEA code and used starting from the PSD stress matrix $\boldsymbol{G}_\sigma(\omega)$ of the element, but it is not tracked by the authors in any of the most commonly used codes.

$$\boldsymbol{G}_\sigma(\omega) = \begin{bmatrix} S_{x,x}(\omega) & S_{x,y}(\omega) & S_{x,z}(\omega) & S_{x,xy}(\omega) & S_{x,xz}(\omega) & S_{x,yz}(\omega) \\ S_{y,x}(\omega) & S_{y,y}(\omega) & S_{y,z}(\omega) & S_{y,xy}(\omega) & S_{y,xz}(\omega) & S_{y,yz}(\omega) \\ S_{z,x}(\omega) & S_{z,y}(\omega) & S_{z,z}(\omega) & S_{z,xy}(\omega) & S_{z,xz}(\omega) & S_{z,yz}(\omega) \\ S_{xy,x}(\omega) & S_{xy,y}(\omega) & S_{xy,z}(\omega) & S_{xy,xy}(\omega) & S_{xy,xz}(\omega) & S_{xy,yz}(\omega) \\ S_{xz,x}(\omega) & S_{xz,y}(\omega) & S_{xz,z}(\omega) & S_{xz,xy}(\omega) & S_{xz,xz}(\omega) & S_{xz,yz}(\omega) \\ S_{yz,x}(\omega) & S_{yz,y}(\omega) & S_{yz,z}(\omega) & S_{yz,xy}(\omega) & S_{yz,xz}(\omega) & S_{yz,yz}(\omega) \end{bmatrix} \tag{20}$$

$$\boldsymbol{s} = \left\{ \quad s_x \quad s_y \quad s_z \quad s_{xy} \quad s_{xz} \quad s_{yz} \quad \right\} \tag{21}$$

The PSD function of the *equivalent von Mises stress* of *Preumont*, G_{EQVM}, is shown by the following relation:

$$G_{EQVM} = trace(\boldsymbol{Q}_\sigma \cdot \boldsymbol{G}_\sigma) \tag{22}$$

where $\boldsymbol{Q}_\sigma$ is:

$$\boldsymbol{Q}_\sigma = \begin{bmatrix} 1 & -1/2 & -1/2 & & & \\ -1/2 & 1 & -1/2 & & & \\ -1/2 & -1/2 & 1 & & & \\ & & & 3 & & \\ & & & & 3 & \\ & & & & & 3 \end{bmatrix} \tag{23}$$

3. Proposed procedure for damage estimation

The principal aim of the paper is to assess the elements damage by avoiding to evaluate $\boldsymbol{G}_\sigma$ matrix for each one but by only analyzing, from a statistical point of view, PSD matrix $\boldsymbol{G}_q$ and, where it is necessary, PSD matrix $\boldsymbol{G}_x$. This would allow to considerably speed up the damage evaluation process and, therefore, to emphasize and disseminate the frequency approach as fatigue assessment tool very useful in the first phase of the design process. In previous work [18,39] the authors had begun to walk this road with good results but having to accept a not always negligible margin of error on the evaluation of the damage.

If motion input condition is considered the stress PSD matrix of the j-th element is provided by (8).

To better understand the following steps an uniaxial stress condition is considered, that is, the $\boldsymbol{G}_\sigma$ matrix has a single component, represented by the power spectral density function G_σ. In this case the spectral moments of the PSD function are evaluable by the following equation (12).

$$\begin{aligned} m_n &= \int_0^\infty G_\sigma f^n df = \\ &= \boldsymbol{\Phi}^\sigma \cdot \left[\int_0^\infty Re(\boldsymbol{G}_q) f^n\, df\right] \cdot (\boldsymbol{\Phi}^\sigma)^{\mathrm{T}} + \boldsymbol{\Phi}_{\mathrm{C}}^\sigma \cdot \left[\int \frac{Re(\boldsymbol{G}_x)}{\omega^4} f^n df\right] \cdot (\boldsymbol{\Phi}_{\mathrm{C}}^\sigma)^{\mathrm{T}} - \\ &- \boldsymbol{\Phi}^\sigma \cdot \left[\int Re(\boldsymbol{H}_q \cdot \frac{\boldsymbol{G}_x}{\omega^2}) f^n df\right] \cdot (\boldsymbol{\Phi}_{\mathrm{C}}^\sigma)^{\mathrm{T}} - \boldsymbol{\Phi}_{\mathrm{C}}^\sigma \cdot \left[\int Re\left(\frac{\boldsymbol{G}_x}{\omega^2} \cdot (\overline{\boldsymbol{H}}_q)^{\mathrm{T}}\right) f^n df\right] \cdot (\boldsymbol{\Phi}^\sigma)^{\mathrm{T}} \end{aligned} \tag{12}$$

where the symbol $Re(\cdot)$ is the "*real part*" operator. Only real parts of all the terms are considered because G_σ itself is real and result of a linear combination of real terms (the real part of the linear combination is equal to the combination of the real parts).

In the case of multiaxial stress condition, if the *Preumont* approach is adopted, it is possible to demonstrate the following relationship:

$$\begin{aligned} m_n &= \int_0^\infty G_{EQVM} f^n df = \\ &= trace\Bigg(\boldsymbol{Q}_\sigma \cdot \Bigg\{\boldsymbol{\Phi}^\sigma \cdot \left[\int_0^\infty Re(\boldsymbol{G}_q) f^n\, df\right] \cdot (\boldsymbol{\Phi}^\sigma)^{\mathrm{T}} + \boldsymbol{\Phi}_{\mathrm{C}}^\sigma \cdot \left[\int \frac{Re(\boldsymbol{G}_x)}{\omega^4} f^n df\right] \cdot (\boldsymbol{\Phi}_{\mathrm{C}}^\sigma)^{\mathrm{T}} - \\ &- \boldsymbol{\Phi}^\sigma \cdot \left[\int Re(\boldsymbol{H}_q \cdot \frac{\boldsymbol{G}_x}{\omega^2}) f^n df\right] \cdot (\boldsymbol{\Phi}_{\mathrm{C}}^\sigma)^{\mathrm{T}} - \boldsymbol{\Phi}_{\mathrm{C}}^\sigma \cdot \left[\int Re\left(\frac{\boldsymbol{G}_x}{\omega^2} \cdot (\overline{\boldsymbol{H}}_q)^{\mathrm{T}}\right) f^n df\right] \cdot (\boldsymbol{\Phi}^\sigma)^{\mathrm{T}}\Bigg\}\Bigg) \end{aligned} \tag{13}$$

that is obtainable by considering the following relation:

$$m_n = \int_0^\infty G_{EQVM} f^n df = trace(\boldsymbol{Q}_\sigma \cdot [\int_0^\infty Re(\boldsymbol{G}_\sigma) f^n df]) \tag{14}$$

In (14) it is sufficient to take the real parts of the $\boldsymbol{G}_\sigma$ because the trace operator contains terms such as: $(Q_\sigma)_{ij} \cdot (G_\sigma)_{ij} + (Q_\sigma)_{ji} \cdot (G_\sigma)_{ji}$. Because of symmetry conditions $(Q_\sigma)_{ij} = (Q_\sigma)_{ji}$ and $(G_\sigma)_{ij} = (\bar{G}_\sigma)_{ji}$ the previous sum is only real. It can be concluded that the imaginary parts of the stress cross-spectra do not affect the values of m_n. Furthermore, it should be noted that the real part of $\boldsymbol{G}_\sigma$, linear combination of matrices, is a linear combination of the real parts of matrices $\boldsymbol{\Theta}_n$, $\boldsymbol{\Lambda}_n$, $\boldsymbol{\Psi}_n$ end $\boldsymbol{\Gamma}_n$, introduced below (15).

The equation (13) could be rewritten as the following equation (15):

$$m_n = trace(\boldsymbol{Q}_\sigma \cdot \{\boldsymbol{\Phi}^\sigma \cdot \boldsymbol{\Theta}_n \cdot (\boldsymbol{\Phi}^\sigma)^T + \boldsymbol{\Phi}_C^\sigma \cdot \boldsymbol{\Lambda}_n \cdot (\boldsymbol{\Phi}_C^\sigma)^T - \boldsymbol{\Phi}^\sigma \cdot \boldsymbol{\Psi}_n \cdot (\boldsymbol{\Phi}_C^\sigma)^T - \boldsymbol{\Phi}_C^\sigma \cdot \boldsymbol{\Gamma}_n \cdot (\boldsymbol{\Phi}^\sigma)^T\}) \tag{15}$$

in which the matrices $\boldsymbol{\Theta}_n$, $\boldsymbol{\Lambda}_n$, $\boldsymbol{\Psi}_n$ and $\boldsymbol{\Gamma}_n$ (named *spectral matrices*, of n order) are evaluated only once (16), by not considering the j-th element that has to be processed but only the system outputs (that is the *Lagrangian coordinates*) and, in general, the inputs characteristics.

$$\boldsymbol{\Theta}_n = \int_0^\infty Re(\boldsymbol{G}_q) f^n\, df \tag{16}$$

$$\mathbf{\Lambda}_n = \int \frac{Re(\boldsymbol{G}_x)}{\omega^4} f^n df$$
$$\mathbf{\Psi}_n = \int Re(\boldsymbol{H}_q \cdot \frac{\boldsymbol{G}_x}{\omega^2}) f^n df$$
$$\mathbf{\Gamma}_n = \int Re\left(\frac{\boldsymbol{G}_x}{\omega^2} \cdot \left(\overline{\boldsymbol{H}}_q\right)^{\mathrm{T}}\right) f^n df$$

Finally, it is possible to calculate the spectral moments of stress state without error for each element by using simple matrix operations (see eqn. 15), once these matrices (see eqn. 16) are evaluated.

It is worth to note that the described approach can be used for every multiaxial criterion (i.e. *critical plane*) that is used to evaluate a single real PSD function of the stress by linear operations between $\boldsymbol{G}_\sigma$ components. The choice of *Preumont's* was done because it gives results with an acceptable error (especially for ductile materials where bending and torsion fatigue curves have the same reverse slope and fatigue strength is scaled by $\sqrt{3}$) [36-38].

This procedure speeds up the calculation because the number of integrals (spectral moments) I to be calculated is reduced. If the model has N elements, m *modal coordinates*, and z inputs, the number of integrations needed for damage calculation by the proposed approach is given by the following relation:

$$I = n \cdot (z^2 + m^2 + 2 \cdot z \cdot m) \tag{17}$$

where n is the number of spectral moment needed for the adopted frequency method (i.e. $n = 4$ for *Dirlik's criterion* and $n = 1$ for *Bands method* [22].). The computational time is reduced as the following inequality shows:

$$n \cdot (z^2 + m^2 + 2 \cdot z \cdot m) \ll n \cdot N \tag{18}$$

in which the second terms represents the number of integrations needed by the classical and reference approach.

The equation (18) is satisfied because $z \ll N$ and $m \ll N$. For example if $z = 10$ inputs, $m = 50$ normal modes and $N = 10^6$ elements are considered, the integrals to be evaluated by the proposed approach are $14.4 \cdot 10^3$, while $4 \cdot 10^6$ are those needed by the classical one. Moreover, it has to be considered that the proposed approach needs the evaluation of only $(m \cdot z)$ frequency response functions $H_{q_{ij}}$ and $(m \cdot m)$ PSDs $G_{q_{ij}}$. The standard method needs of $(6\,N \cdot z)$ frequency response functions $H_{\sigma_{ij}}$ and consequently N times $(6 \cdot 6)$ stress PSDs $G_{\sigma ij}$ and N syntheses of these functions into a single PSD function, for example by *von Mises*' rule or *Preumont* approach. So the speed up is much more evident than the only comparison in terms of spectral moments evaluation.

Finally, it has to be highlighted that for force excitation equation (15) becomes:

$$m_n = trace(\boldsymbol{Q}_\sigma \cdot \{\mathbf{\Phi}^\sigma \cdot \mathbf{\Theta}_n \cdot (\mathbf{\Phi}^\sigma)^{\mathrm{T}}\}) \tag{19}$$

For this kind of problems the proposed approach is faster because the integrals to be calculated are $(n \cdot m^2)$ and equation (18) becomes:

$$n \cdot m^2 \ll n \cdot N \tag{20}$$

If the previous example is considered, only $1 \cdot 10^4$ integrals have to be evaluated instead of $4 \cdot 10^6$.

It is worth noting that the proposed approach is a clever rewriting of the classical approach and therefore does not cause any error or approximation with respect to the standard procedure, shown in the previous section. In figure 1 the flow chart of the proposed procedure is compared with that of the classical approach.

4. Damage evaluation procedures

In the present paper two test cases are analyzed and two fatigue damage evaluation procedures are used: *Dirlik*'s method [3] and *Bands method* [22]. The first approach is based on four spectral moments and the second one on only one of these. The first method is, moreover, the standard for a great number of researcher and in this case too represents the referment point for the judge on the others frequency domain approacches.

Obviously, starting from the exact evaluation of the stress PSD function spectral moments, all the frequency domain criteria based on spectral moments are adoptable.

Equation (21) shows Dirlik's approach.

$$f_\sigma(\Delta\sigma) = \frac{\frac{D_1}{Q} e^{(-Z/Q)} + \frac{D_2 Q}{R^2} e^{-(Q^2/(2R^2))} + D_3 Z e^{(-Q^2/2)}}{2\sqrt{m_0}} \tag{21}$$

where:

$\gamma = m_2/\sqrt{m_0 m_4}$,

$Z = \Delta\sigma/\left(2\sqrt{m_0}\right)$,

$x_m = (m_1/m_0)\sqrt{m_2/m_4}$,

$D_1 = [2(x_m - \gamma^2)]/(1+\gamma^2)$

$R = \left(\gamma - x_m - {D_1}^2\right)/\left(1 - \gamma - D_1 + {D_1}^2\right)$,

$D_2 = \left(1 - \gamma - D_1 - {D_1}^2\right)/(1 - R)$,

$D_3 = (1 - D_1 - D_2)$,

$Q = 1.25 \cdot (\gamma - D_3 - D_2 R)/D_1$

From the knowledge of the stress range probability density function and of the fatigue strength curve of the material (i.e. in the stress/cycles domain, S-N) [38], it is possible to calculate the fatigue damage by employing a cumulative damage law (i.e. linear cumulative damage law) [38].

By adopting, for the S-N curve, the following relation (22):

$$\Delta\sigma^k = \frac{C}{N} \tag{22}$$

and knowing the probability density function of the stress range, is possible to write the fatigue damage D by relation (23):

$$D = \frac{T \cdot n_t}{C} \int_0^\infty (\Delta\sigma)^k \cdot f_\sigma(\Delta\sigma)\, d(\Delta\sigma) \tag{23}$$

where n_t is the number of cycles per time unit, that it is equal to $\nu_p = \sqrt{\frac{m_4}{m_2}}$ and T is the duration of random signal application characterized by the assigned PSD function.

The second one was developed by authors [22] to speed up the damage evaluation step by using only the first spectral moment of the stress PSD function. *Braccesi* et al. in [22] proposed a method to estimate the fatigue damage of a wide-band random process in the frequency domain. It is based on the same starting idea of *Benasciutti*'s one [36-38] (even if developed and applied in different application scenarios, i.e. uniaxial and multiaxial conditions) that is on the decomposition of a Power Spectral Density (PSD) into narrow-band frequency components, sufficiently narrow to be associated to a Rayleigh distribution of stress cycles amplitude.

From a procedural point of view if the Power Spectral Density function is divided into m bands, each i-th band characterized by a central frequency f_i, m Narrow Band independent random variables are obtained. Each band and the relative random process has a different cycles numerousness, function of f_i. The combination of the m processes is possible only if these processes have the same cycles numerousness. In order to obtain this condition, the bands, that is the relative central frequencies (f_i), are "moved" to an arbitrary reference band, that is to a reference central frequency (f_{ref}).

By performing this operation, m Narrow Band independent random processes, that takes place at the same frequency, are obtained. The distribution of cycles of the combination process will then be a Rayleigh distribution, with a cycles number equal to the reference frequency f_{ref}.

The formulation of the total fatigue damage is given for this approach by the following:

$$D = \frac{K \cdot \alpha^{\frac{1}{\beta}} \cdot f_{ref}}{\left(\int G_{ref}(f)df\right)^{1/2\beta}} \tag{24}$$

in which:

$$G_{ref}(f) = \left(\frac{f_{ref}}{f}\right)^{2\beta} G(f) \tag{25}$$

being K the Γ function and α and β parameters of the *Wöhler*'s curve, expressed in Eq. (26):

$$N = \left(\frac{\sigma_a}{\alpha}\right)^{1/\beta} \tag{26}$$

where N is the number of loading cycles, σ_a is the amplitude of the applied loading ($\sigma_a = 1/2 \cdot \Delta\sigma$), β is the curve slope and α is the curve intercept.

The advantage of the this formulation lies, however, in its simplicity: it is sufficient to correct the original Power Spectral Density function with a coefficient that depends on the frequency and to calculate the PSD area to evaluate the damage.

5. Test cases

To demonstrate the efficiency of the proposed modal procedure two FE models were analyzed.

The models were built by a commercial FE code (HyperMesh©).

As first example, a simple portal was considered [24]. A 2D model of the structure was realized, by using shell elements with 3 or 4 nodes and 3 *dofs* per node, characterized by 4791 elements, 5283 nodes, 15849 *dofs*, clamped to the lower extremes (fig.2). It is a 1.0 × 1.0 m portal with beams width of 0.6 m and thickness of 4 mm, realized in aluminum alloy, with elastic modulus of $0.7 \cdot 10^{11}$ N/m^2 and mass density of 2600 kg/m^3.

A single point motion base load condition is considered. An acceleration PSD function was applied to load *dofs* along *y* direction (fig. 2). It is a flat PSD with constant amplitude of 83.13 (g^2/Hz) between 10 to 2000 Hz (fig.3). A modal coordinates subset of 10 modes is considered (in figure 4, left column, the first four mode shapes are shown; in table 1 the relative natural frequencies are reported). A *Wöhler* curve $S = \alpha N^{\beta}$ was adopted, in which S represents the alternating stress component and N the number of cycles to failure. The strength curve of the choose material is characterized by a single constant slope. The material's constants are $\alpha = 800$ MPa, and $\beta = -0.10$.

The reference procedure and the proposed one were performed in MATLAB© starting by input PSD and FEA intermediate results as previously defined.

The comparison, first of all, was performed in terms of spectral moments of the equivalent stress PSD function for each element and, then, in terms of damage. As theoretically demonstrated, a zero error is measured in the evaluation of all moments of each element. This means that zero error is obtainable for damage evaluation by adopting whatever damage evaluation methods based on spectral moments.

In order to allow to verify this affirmation the stress state of a single element (ID 1678) is analyzed. This element is the most damageable. The stress PSD of this element, obtainable by the standard approach [39,26] (see paragraph no.2), is represented in figure 5. In table 2 the relative spectral moments are reported. In table 3 the spectral moments of PSD matrix of *Lagrangian* coordinates of the model are reported and in figure 6 some functions of the first modal coordinates are represented. Moreover, in table 4 the modal stress shapes of the above element are shown. From these data ($\boldsymbol{G}_q$ and $\boldsymbol{\Phi}^{\sigma}$) is possible to immediately recover the same stress spectral moments of the first row of table 2 by the relation (19), as it is observable in the second row of the same table, verifying the goodness of the previous affirmation.

The analysis of results shows that the difference between the reference approach and the proposed one is evident in terms of computation time. For this test case $z = 1$, $m = 10$ and $N = 4791$, and equation (20) shows that the integrals to be evaluated by the proposed approach to obtain the stress spectral moments for all the elements are 400 or 100 respectively if *Dirlik*'s ($n = 4$) or *Bands* method is used ($n = 1$), while 19164 are those needed by the reference one.

Consequently, the damage of the whole model was evaluated both by *Dirlik*'s and *Bands* method and adopting *Miner*'s rule to obtain damage by S–N fatigue approach. This constitutes an ulterior test bench for the *Bands method*, compared to the "standard" approach (*Dirlik*'s).

In terms of computational time (see table 5) this means that to obtain the damage for the whole model the reference approach plus *Dirlik*'s method needs 196 s (about three minutes) and the proposed one, plus *Dirlik*'s method too, 0.9 s, two hundred times faster. Moreover, if *Bands method* is used the computational times decreases to 0.2 s, one thousand times faster.

This ratio becomes more significant if translated into industrial test case as the following example shows. This results also confirms the extremely speeding up of the proposed procedure respect the standard one, obtainable without introducing any error in the evaluation of the stress spectral moments.

As concern, instead, the comparison between *Dirlik*'s and *Bands* method, figure 7 shows a comparison in terms of absolute damage values. Damage maps are overlapping both in a global and in a local representation, this last focused on the most damageable zone. A numerical comparison is reported in table 6 in which, for the ten most damaged elements, damage values, obtained by the two methods, are shown together with the stress PSD function spectral moments.

As second example, a pedestrian bridge was considered. A 3D model was realized (fig. 8), by using shell elements with 3 or 4 nodes and 6 *dofs* per node, characterized by 77333 elements, 79932 nodes, 479592 *dofs*, constrained as figure 8 shows. It is a 4.0 × 0.92 × 0.80 m bridge, realized in steel, with elastic modulus of $2.1{\cdot}10^{11}$ N/m^2 and mass density of 7800 kg/m^3.

A single point motion base load condition is considered. An acceleration PSD function was applied to load *dofs* along *y* direction (see figure 9) in a range between 3 to 500 Hz. A modal coordinates subset of 15 modes is considered (in figure 4, right column, the first four mode shapes are shown; in table 1 the relative natural frequencies are reported). A *Wöhler* curve $S = \alpha N^{\beta}$ was adopted, in which S represents the alternating stress component and N the number of cycles to failure. The strength curve of the chosen material is characterized by a single constant slope. The material's constants are $\alpha = 556$ MPa, and $\beta = -0.084$.

As for the previous test case, the reference procedure and the proposed one were performed in MATLAB© starting by input PSD and FEA intermediate results, as previously defined.

Also for this example, the comparison was performed in terms of spectral moments of the equivalent stress PSD function for each element and then in terms of damage. Zero error is measured in the evaluation of all the moments of each element.

The stress state of the most damageable element (ID 67357) is analyzed. The stress PSD of this element, obtainable by the standard approach, is represented in figure 10. In table 7 the relative spectral moments are reported. In table 8 the spectral moments of PSD matrix of *Lagrangian coordinates* of the model are reported and in figure 11 some functions of the first modal coordinates are represented. Moreover, in table 9 the modal stress shapes of the above element are shown. From these data ($\boldsymbol{G}_q$ and $\boldsymbol{\Phi}^{\sigma}$) is possible to immediately recover by eqn. (18), the same stress spectral moments obtainable by reference approach, as it is observable in table 7.

The analysis of results shows that the difference between the reference approach and the proposed one is evident in terms of computational time. For this test case $z = 1$, $m = 15$ and $N = 77333$, and equation (20) shows that the integrals to be evaluated by the proposed approach to obtain the stress spectral moments for all the elements are 900 or 225 respectively if *Dirlik*'s ($n = 4$) or *Bands* method is used ($n = 1$), while 309332 are those needed by the reference one.

Consequently, the damage of the whole model was evaluated both by *Dirlik*'s and *Bands* method and adopting *Miner*'s rule to obtain damage by S–N fatigue approach. This constitutes an ulterior test bench for the *Bands method,* compared to the "standard" approach (*Dirlik*'s).

In terms of computation time (see table 10) this means that to obtain the damage for all model the reference approach plus *Dirlik*'s method needs 1594 s (about half an hour) and the proposed one, plus *Dirlik*'s method too, 13.3 s, one hundred times faster. Moreover, if *Bands method* is used the computational times decreases to 1.7 s, nine hundred times faster.

This results also confirms the extremely speeding up of the proposed procedure especially if combined with the adoption of a frequency domain evaluation method that use few spectral moments (i.e. *Bands method*).

As concern, instead, the comparison between damage maps, obtained by *Dirlik*'s and *Bands* method, figures 12 and 13, it shows the overlapping of them, both in a global and in a local representation, this last focused on the most damageable zone. A numerical comparison is reported in table 11 in which, for the ten most damaged elements, damage values, obtained by the two methods, are shown together with the stress PSD function spectral moments.

6. Conclusions

In this paper an innovative procedure, developed by authors to obtain exact values of spectral moments of stress PSD functions of a generic finite element model modelled by modal approach, is shown. The innovation consists in a smart use of the *Lagrangian coordinates* and inputs PSD functions matrices that very deeply accelerates the evaluation process, determining a speeding up that reduces the standard computational times among four and nine hundred times.

Starting from PSD input matrix, intermediate frequency analysis results, such as PSD matrix of *Lagrangian coordinates* and stress shapes of normal and constraint modes, it is possible to obtain the exact values of the stress spectral moments of all elements and, by adopting whatever direct frequency domain approach based on these, the exact values of the fatigue damage. This procedure is very fast and easily implementable in any commercial FE codes.

In this paper a detailed verification of this approach is shown. By using two different structures and relative FE models the efficiency of the above procedure and of some frequency domain damage evaluation methods was verified both in terms of damage and of computational times. In particular, a new frequency domain method, proposed by authors in a previous paper, was compared to the consolidated *Dirlik*'s one. The comparison has shown the goodness of it, especially in terms of computational times.

References

[1] P.H. Wirsching, M.C. Light, Fatigue under wide band random stresses, J. Struct. Div. ASCE, vol. 106(ST7), pp. 1593–607, 1980.

[2] J.S. Bendat, A.G. Piersol, Random data, analysis and measurement procedure, Third Edition", A Wiley Interscience publication, 1986.

[3] T. Dirlik, Application of computers in fatigue analysis, University of Warwick Thesis, 1985.

[4] A. Preumont, V. Piefort, Predicting random high-cycle fatigue life with finite elements, Journal of Vibration and Acoustics, Transactions of the ASME, 116(2), pp. 245-248, 1994.

[5] D.P. Kihl, S. Sarkani, J.E.Beach, Stochastic fatigue damage accumulation under broadband loadings, Int. J. Fatigue, vol. 17 (5), pp. 321-329, 1995.

[6] N.W.M. Bishop, F. Sherratt, A theoretical solution for the estimation of Rainflow ranges from power spectral density data, Fatigue Fracture Engineering Material, 13(4), pp. 311-326, 1990.

[7] L.D. Lutes, C.E. Larsen, An improved spectral method for variable amplitude fatigue prediction, J. Struct. Div. ASCE, 116, pp. 1149-1164, 1990.

[8] S. Sakai, H. Okamura, On the distribution of rainflow range for gaussian random processes with bimodal PSD, JSME Int. J., Series A, vol. 38(4), pp. 440-445, 1995.

[9] G. Petrucci, G. Di Paola, B. Zuccarello, On The Characterization Of The Dynamic Properties of Random Processes by Spectral Parameters,. J. of Applied Mechanics, vol. 67(3), pp. 519-526, 2000.

[10] G. Petrucci, B. Zuccarello, Fatigue Life Prediction Under Wide Band Random Loading, Int. J. Fatigue, vol. 27(12), pp. 1183-1195, 2004

[11] C. Braccesi, F. Cianetti, G. Lori, D. Pioli, Fatigue behaviour analysis of mechanical components subject to random bimodal stress process: frequency domain approach, Int. J. Fatigue, vol. 27(4), pp.335-345, 2005.
[12] C. Braccesi, F. Cianetti, G. Lori, D. Pioli, A frequency method for fatigue life estimation of mechanical components under bimodal random stress process, Structural Integrity Durability, vol. 1(4), pp. 277-290, 2005.
[13] M. Wang, W. Yao, Frequency domain method for fatigue life analysis on notched specimens under random vibration loading, Journal of Nanjing University of Aeronautics and Astronautics, vol. 40 (4), pp. 489-492, 2008.
[14] C. Braccesi, F. Cianetti, G. Lori, D. Pioli, The frequency domain approach in virtual fatigue estimation of non-linear systems: The problem of non-Gaussian states of stress, Int. J. Fatigue, vol. 31 (4), pp. 766-775, 2009.
[15] T.E. Putra, S. Abdullah, M.Z. Nuawi, Data scattering of fatigue damaging segmentation in order to develop the fatigue damaging and Morlet wavelet coefficient relationship, Int. Review of Mechanical Engineering, vol. 5 (4), pp. 605-610, 2011.
[16] C. Braccesi, F. Cianetti, Random loads fatigue and dynamic simulation: A new procedure to evaluate the behaviour of non-linear systems, SDHM Structural Durability and Health Monitoring, vol. 7(1-2), pp. 83-116, 2011.
[17] N. Takeda, T. Naruse, Accurate prediction of fatigue life under random loading, Journal of the Society of Materials Science, vol. 61 (10), pp. 853-859, 2012
[18] F. Cianetti, Development of a modal approach for the fatigue damage evaluation of mechanical components subjected to random loads, SDHM Structural Durability and Health Monitoring, vol. 8(1), pp. 1-29, 2012.
[19] K. Walat, Selection of the best method for assessment of the fatigue life of aluminium alloys based on the root of the scatter mean-square value, Acta Mechanica et Automatica, vol. 6 (1), pp. 86-88, 2012.
[20] M. Mršnik, J. Slavič, M. Boltežar, “Frequency-domain methods for a vibration-fatigue-life estimation. Application to real data”, Int. J. Fatigue, vol. 7, pp. 8-17, 2013.
[21] C. Braccesi, F. Cianetti, G. Lori, D. Pioli, Evaluation of mechanical component fatigue behavior under random loads: Indirect frequency domain method, Int. J. Fatigue, vol. 61, pp. 141-150, 2014.
[22] C. Braccesi, F. Cianetti, L. Tomassini, Random fatigue. A new frequency domain criterion for the damage evaluation of mechanical components, Int. J. Fatigue, vol. 70, pp. 417-427, 2015.
[23] C.E. Larsen, T. Irvine, A review of spectral methods for variable amplitude fatigue prediction and new results, Proc. Eng., vol. 101, pp. 243-250, 2015.
[24] C. Braccesi, F. Cianetti, L. Tomassini, Validation of a new method for frequency domain dynamic simulation and damage evaluation of mechanical components modelled with modal approach, Proc. Eng., vol. 101, pp. 493-500, 2015.
[25] S.M. Ross, “Probability and statistics for engineers and scientists”, Academic Press, 2000.
[26] A. Preumont, Random vibration and spectral analysis, Kluwer Academic Publishers, 1994.
[27] Lagoda T, Macha E., “Simulation of cross-correlation effect on biaxial random fatigue”, Proceedings of Proceedings of the Fifth International Conference on Fatigue and Fatigue Thresholds held, vol. 3, pp. 1539-1544, Montreal (CAN), 1993.
[28] Lagoda T., Macha E., Dragon A., Petit J., “Influence of correlations between stresses on calculated fatigue life of machine elements”, Int. J. Fatigue, vol. 18(8), pp.547-555, 1996.
[29] X. Pitoiset, A. Preumont, A. Kernilis, Tools for a multiaxial fatigue analysis of structures submitted to random vibrations, Proc. European Conference on Spacecraft Structures materials and Mechanical Testing, 1998.
[30] X. Pitoiset, A. Preumont, Spectral methods for multiaxial random fatigue analysis of metallic structures, Int. J. Fatigue, vol. 22(7), pp. 541-550, 2000.
[31] X. Pitoiset, I. Rychlik, A. Preumont, Spectral methods to estimate local multiaxial fatigue failure for structures undergoing random vibrations, Fatigue and Fracture of Engineering Materials and Structures, vol. 24(11), pp. 715-727, 2001.
[32] A. Nieslony, Comparison of some selected multiaxial fatigue failure criteria dedicated for spectral method, Journal of Theoretical and Applied Mechanics, vol. 48(1), pp. 233-254, 2010.
[33] A. Cristofori, D. Benasciutti, R. Tovo, A stress invariant based spectral method to estimate fatigue life under multiaxial random loading, Int. J. Fatigue, vol. 33(7), pp. 887-899, 2011.
[34] A. Nieslony, M. Ruzicka, J. Papuga, A. Hodr, A. Balda, J. Svoboda, Fatigue life prediction for broad-band multiaxial loading with various PSD curve shapes, Int. J. Fatigue, vol. 44, pp. 74-88, 2012.
[35] C. Braccesi, F. Cianetti, G. Lori, D. Pioli, An equivalent uniaxial stress process for fatigue life estimation of mechanical components under multiaxial stress conditions, Int. J. Fatigue, vol. 30(8), pp. 1479-1497, 2008.
[36] D. Benasciutti, A. Cristofori, R. Tovo, Analogies between spectral methods and multiaxial criteria in fatigue damage evaluation, Prob. Eng. Mech., vol. 31, pp.39-45, 2013.
[37] A. Cristofori, D. Benasciutti, "Projection-by-Projection" approach: a spectral method for multiaxial random fatigue, SAE Technical Paper 2014-01-0924.
[38] J.A. Collins, Failure of materials in mechanical design: analysis, prediction, prevention, Wiley&Sons, New York, 1993.
[39] C. Braccesi, F. Cianetti, L. Landi, Random loads fatigue. the use of spectral methods within multibody simulation, Proceedings of the ASME International Design Engineering Technical Conferences and Computers and Information in Engineering Conference, pp.1735-1745, 2005.
[40] C. Braccesi, F. Cianetti, Development of selection methodologies and procedures of the modal set for the generation of flexible body models for multibody simulation, Proc. of The Institution of Mechanical Engineers Part K - Journal of Multi-Body Dynamics, vol. 218(1), pp. 19-30, 2004.
[41] M.C.C. Bampton, R.R. Craig, Coupling of substructures for dynamic analyses, AIAA Journal, vol. 6(7), pp.1313-1319, 1968

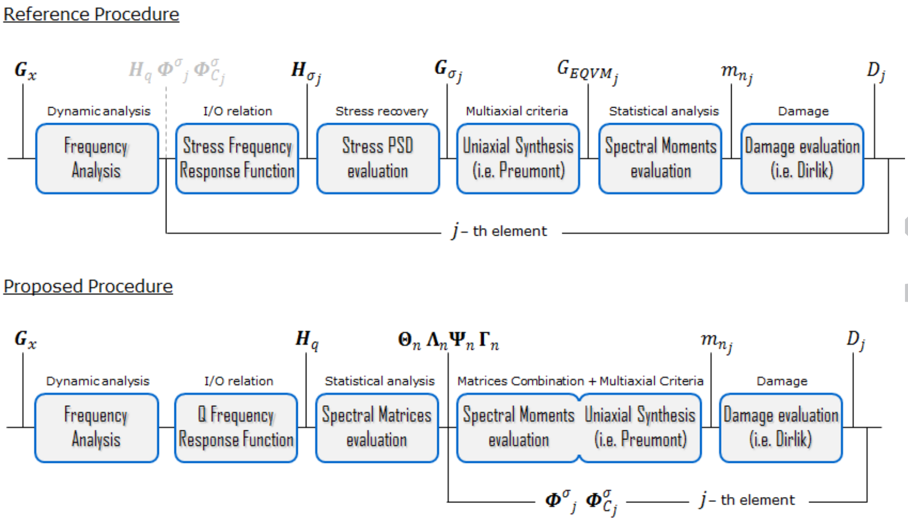

Figure 1 – Comparison between flow charts of reference and proposed procedure

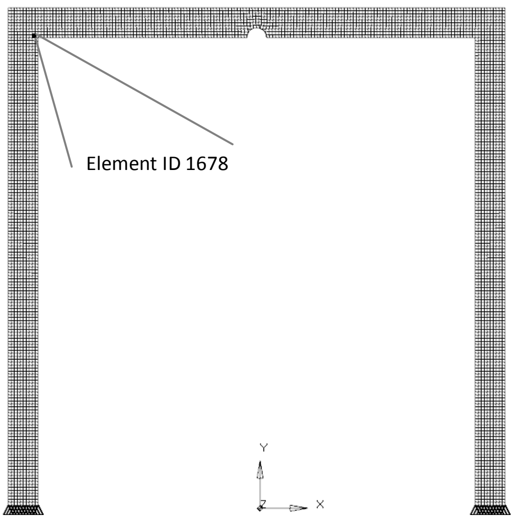

Figure 2 – Representation of FE model of test case no.1 and of the most damageable element (ID = 1678)

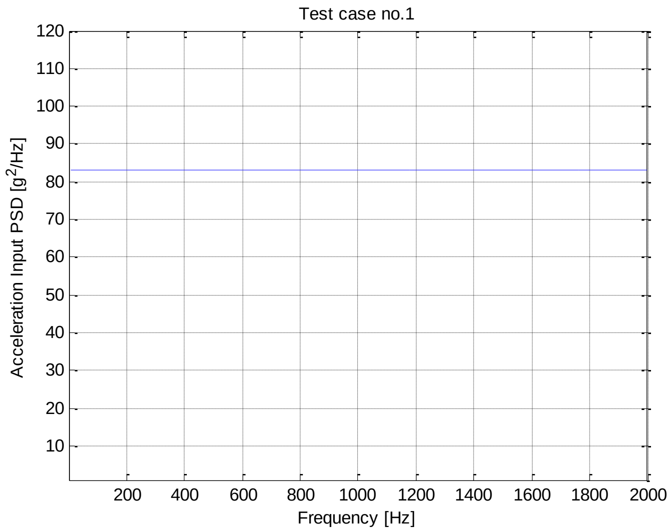

Figure 3 – PSD function of the acceleration input - test case no.1

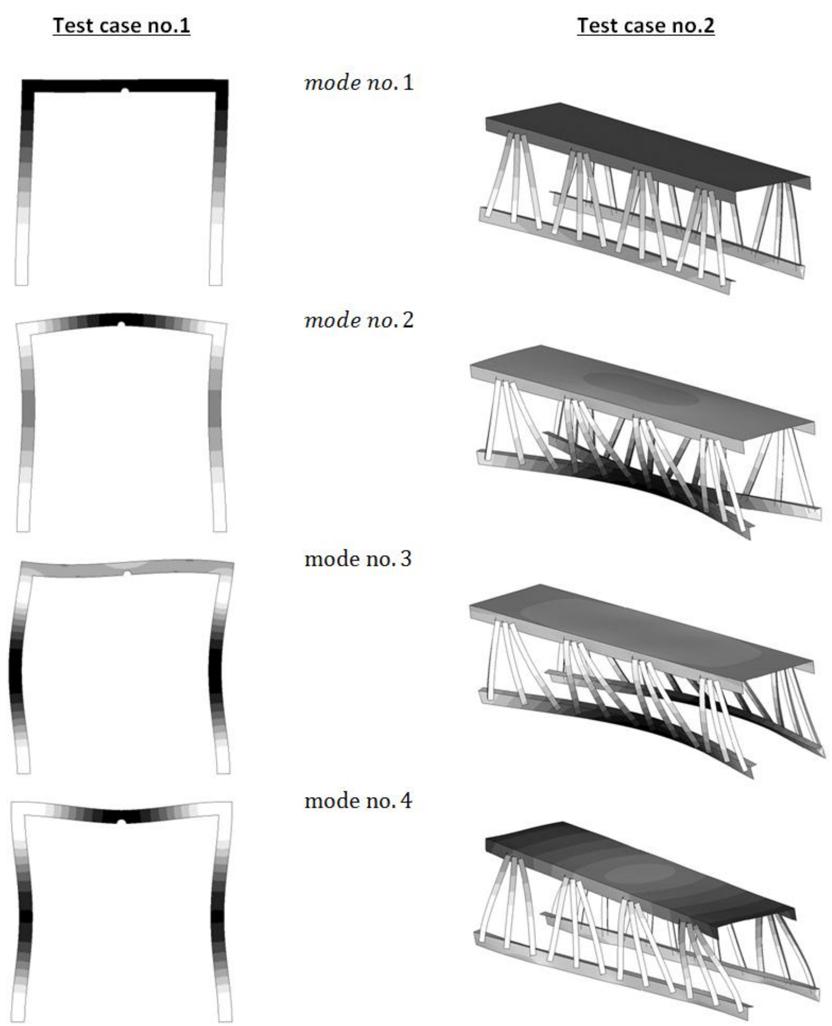

Figure 4 – Mode shapes of FE models (test cases no.1 and no.2)

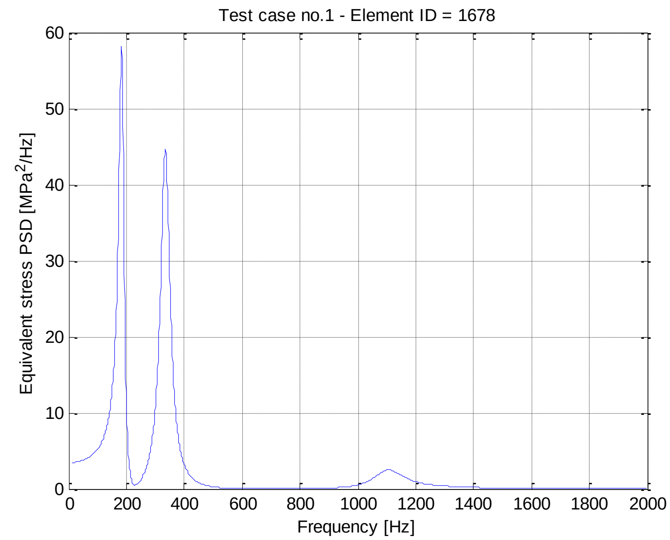

Figure 5 – PSD function of the equivalent stress obtained by standard approach for the most damageable element (ID = 1678) - test case no.1

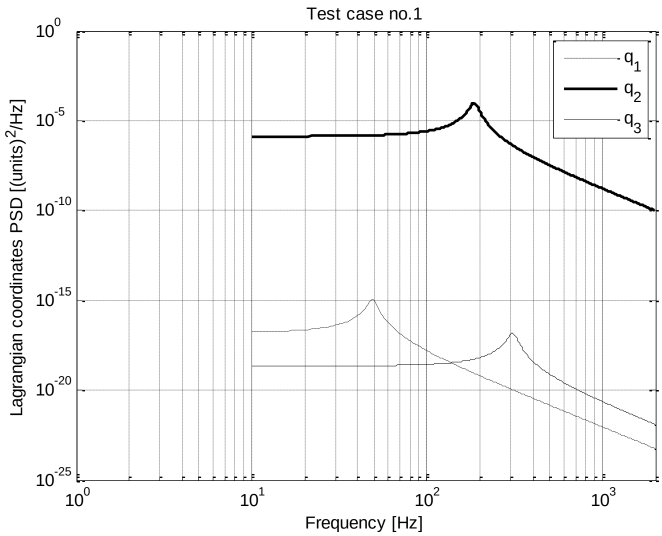

Figure 6 – PSD functions (autospectra) of the first three *Lagrangian* coordinates - test case no.1

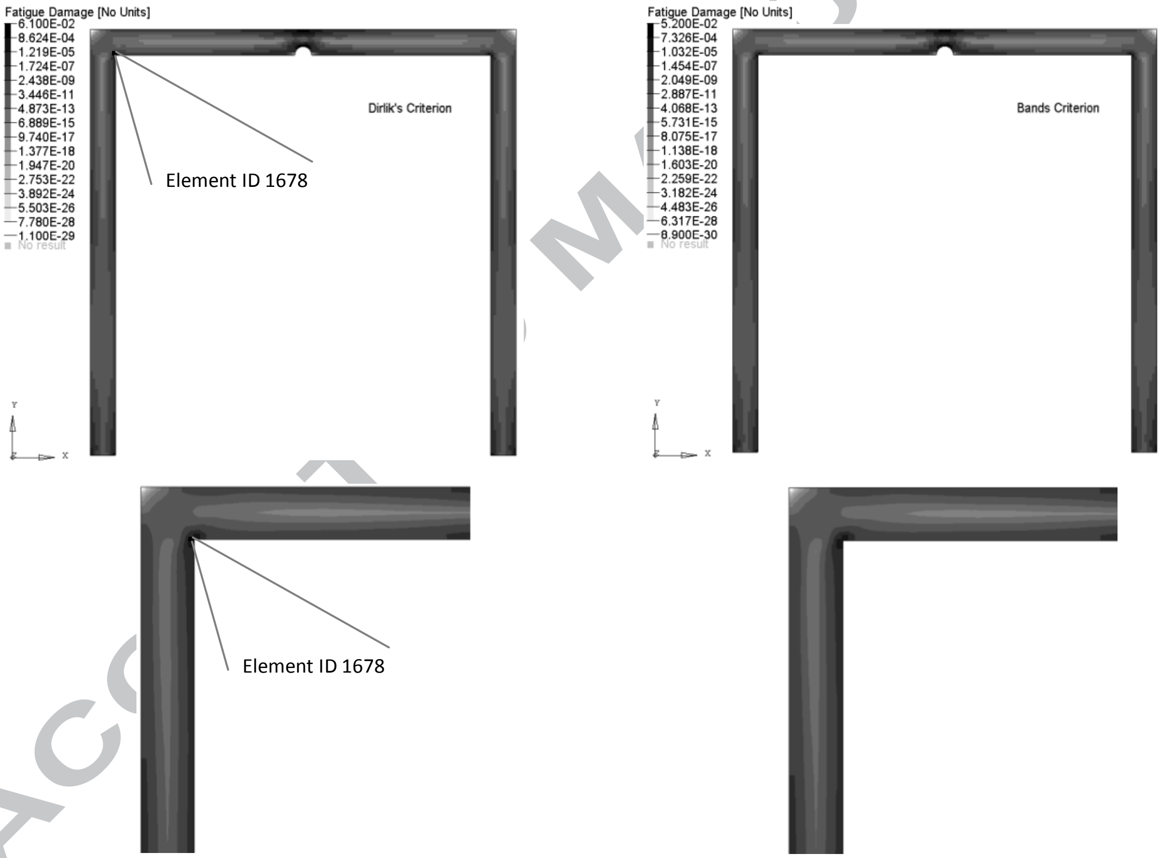

Figure 7 – Comparison in terms of absolute damage values between *Dirlik*'s (left figures) and *Bands* (right figures) method. Damage maps are shown both in a global (upper figures) and in a local (bottom ones) representation, this last focused on the most damageable zone (model upper left corner) - test case no.1

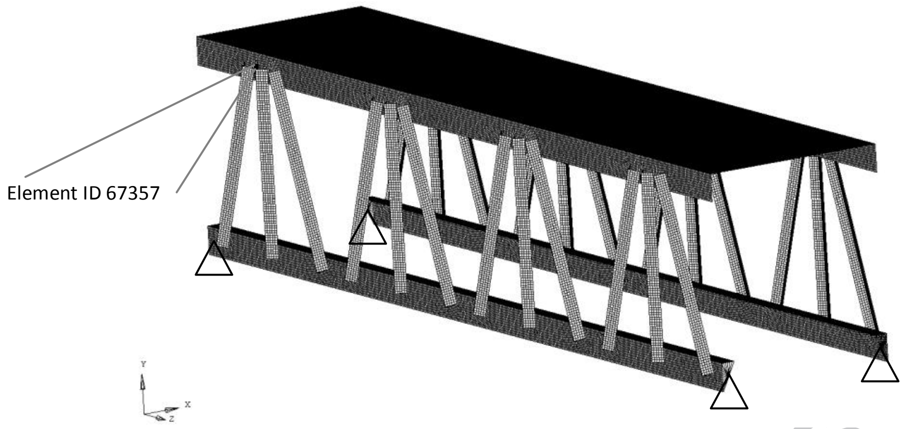

Figure 8 – Representation of FE model of test case no.2 and of the most damageable element (ID = 67357)

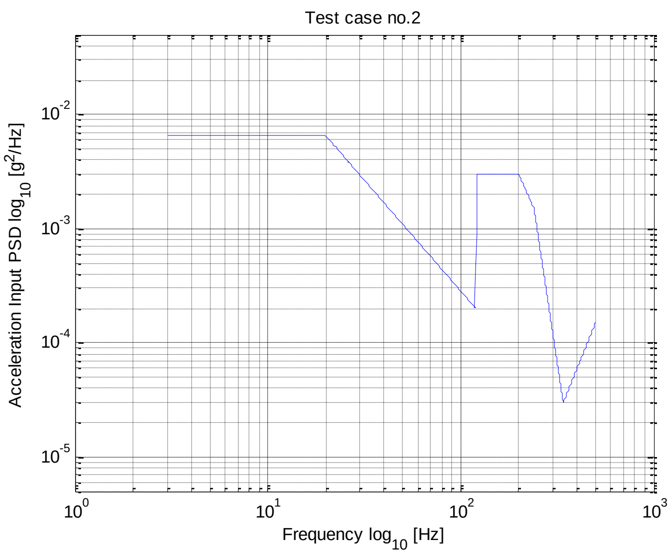

Figure 9 – PSD function of the acceleration input - test case no.2

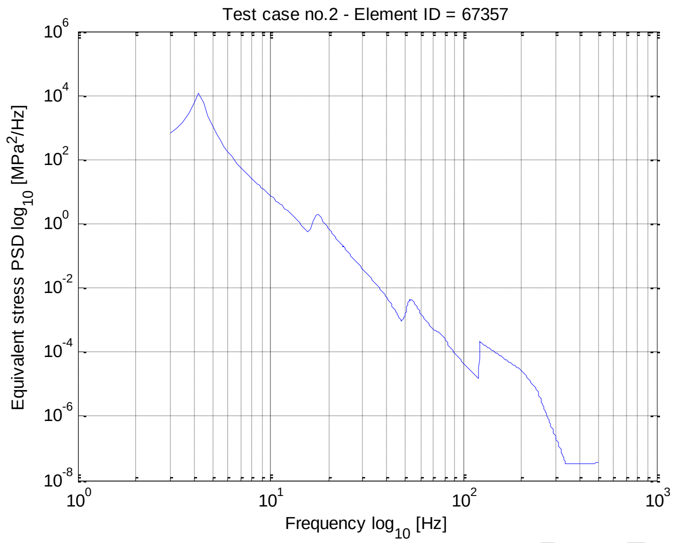

Figure 10 – PSD function of the equivalent stress obtained by standard approach for the most damageable element (ID = 67357) - test case no.2

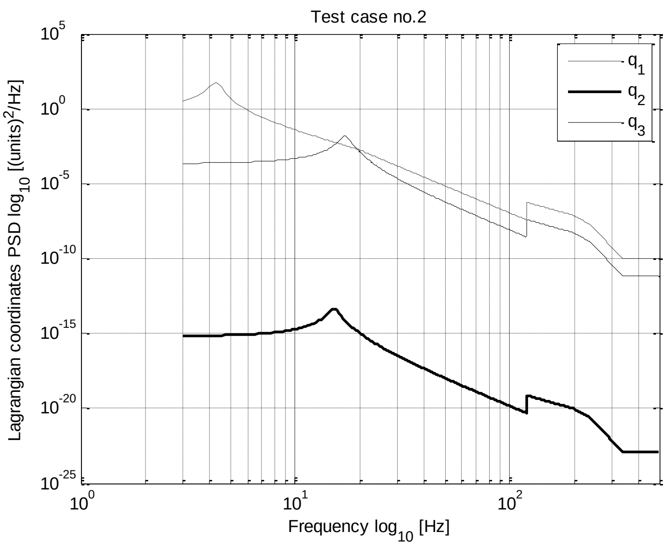

Figure 11 – PSD functions (autospectra) of the first three *Lagrangian* coordinates - test case no.2

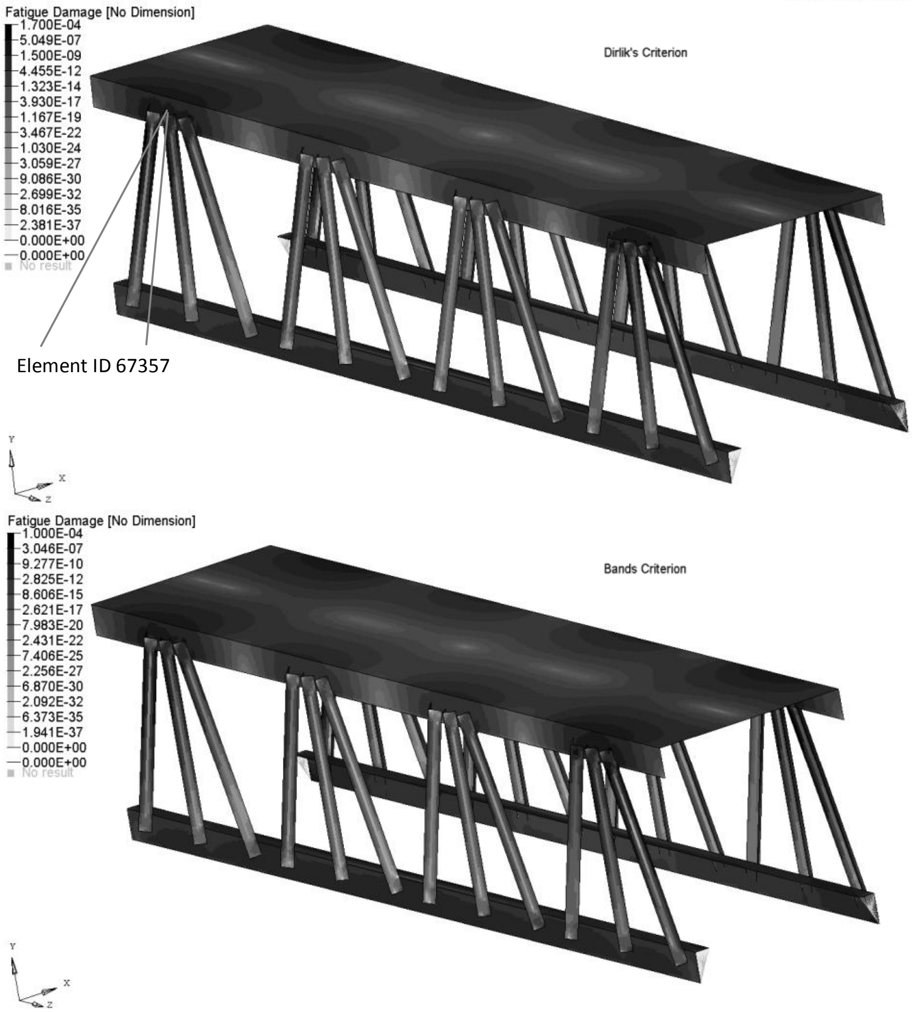

Figure 12 – Comparison in terms of absolute damage values between *Dirlik*'s (upper figure) and *Bands* (bottom figure) method. Damage maps are shown in a global representation - test case no.2

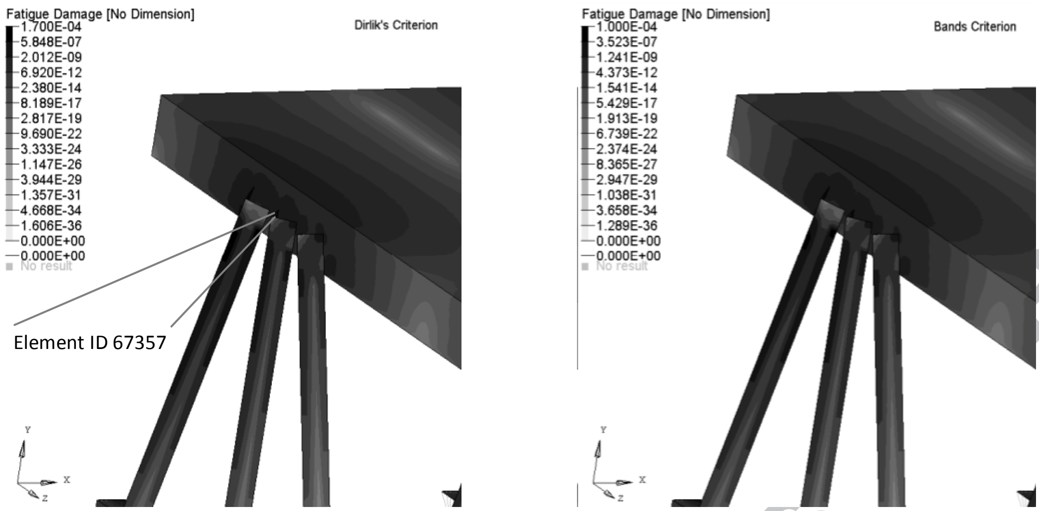

Figure 13 – Comparison in terms of absolute damage values between *Dirlik*'s (left figure) and *Bands* (right figure) method. Damage maps are shown in a local representation, this last focused on the most damageable zone (model upper left structural *node*) - test case no.2

Table 1. Natural Frequencies of FE models (test cases no.1 and no.2)

Procedure type	$mode\ no. 1$ [Hz]	$mode\ no. 2$ [Hz]	$mode\ no. 3$ [Hz]	$mode\ no. 4$ [Hz]
Test case no. 1	48.9	186	308	335
Test case no. 2	4.26	15.20	17.10	32.10

Table 2. Spectral moments of equivalent stress PSD function (Element ID = 1678) – test case no. 1

Procedure type	m_0 [MPa^2]	m_1 [$MPa^2 \cdot Hz$]	m_2 [$MPa^2 \cdot Hz^2$]	m_4 [$MPa^2 \cdot Hz^4$]
Reference Procedure	$2.219 \cdot 10^4$	$7.968 \cdot 10^6$	$5.612 \cdot 10^9$	$6.116 \cdot 10^{15}$
Proposed Procedure	$2.219 \cdot 10^4$	$7.968 \cdot 10^6$	$5.612 \cdot 10^9$	$6.116 \cdot 10^{15}$

Table 3. Spectral moments of PSD matrix of *Lagrangian* coordinates –test case no. 1

m_0	q_1	q_2	q_3	q_4	q_5	q_6	q_7	q_8	q_9	q_{10}
q_1	1.009E-14	-1.444E-11	-1.232E-17	7.368E-12	-1.582E-17	-2.992E-13	-1.374E-17	-2.109E-12	-1.928E-17	-4.479E-13
q_2	-1.444E-11	3.249E-03	8.008E-11	-3.378E-05	9.849E-12	1.115E-07	3.164E-12	1.482E-07	-6.034E-13	-5.104E-08
q_3	-1.232E-17	8.008E-11	8.748E-16	-3.427E-10	2.419E-17	2.836E-13	9.197E-18	8.370E-13	4.704E-18	5.791E-14
q_4	7.368E-12	-3.378E-05	-3.427E-10	3.070E-04	-1.897E-11	-2.161E-07	-6.939E-12	-6.340E-07	-3.658E-12	-4.852E-08
q_5	-1.582E-17	9.849E-12	2.419E-17	-1.897E-11	1.776E-15	1.091E-11	2.062E-16	1.287E-11	6.843E-17	1.010E-12
q_6	-2.992E-13	1.115E-07	2.836E-13	-2.161E-07	1.091E-11	7.121E-07	1.463E-11	6.057E-07	2.775E-12	3.872E-08
q_7	-1.374E-17	3.164E-12	9.197E-18	-6.939E-12	2.062E-16	1.463E-11	1.651E-15	7.202E-11	2.656E-16	3.380E-12
q_8	-2.109E-12	1.482E-07	8.370E-13	-6.340E-07	1.287E-11	6.057E-07	7.202E-11	4.470E-05	1.731E-10	1.689E-06
q_9	-1.928E-17	-6.034E-13	4.704E-18	-3.658E-12	6.843E-17	2.775E-12	2.656E-16	1.731E-10	4.124E-15	5.043E-11
q_{10}	-4.479E-13	-5.104E-08	5.791E-14	-4.852E-08	1.010E-12	3.872E-08	3.380E-12	1.689E-06	5.043E-11	2.392E-06

m_1	q_1	q_2	q_3	q_4	q_5	q_6	q_7	q_8	q_9	q_{10}
q_1	4.828E-13	-1.239E-08	-7.413E-15	4.436E-09	-1.079E-14	-2.142E-10	-1.024E-14	-1.671E-09	-1.605E-14	-3.899E-10
q_2	-1.239E-08	5.832E-01	6.058E-09	-4.271E-04	-1.954E-08	-4.322E-04	-2.208E-08	-3.902E-03	-3.950E-08	-1.000E-03
q_3	-7.413E-15	6.058E-09	2.598E-13	-1.043E-07	-7.836E-15	-2.577E-10	-1.510E-14	-2.993E-09	-3.208E-14	-8.448E-10
q_4	4.436E-09	-4.271E-04	-1.043E-07	9.931E-02	2.968E-09	1.423E-04	8.947E-09	1.853E-03	2.023E-08	5.383E-04
q_5	-1.079E-14	-1.954E-08	-7.836E-15	2.968E-09	1.128E-12	6.864E-09	1.066E-13	1.265E-09	-3.875E-14	-1.653E-09
q_6	-2.142E-10	-4.322E-04	-2.577E-10	1.423E-04	6.864E-09	5.399E-04	1.119E-08	3.419E-04	4.255E-10	-2.054E-05
q_7	-1.024E-14	-2.208E-08	-1.510E-14	8.947E-09	1.066E-13	1.119E-08	1.435E-12	6.013E-08	1.586E-13	5.077E-10
q_8	-1.671E-09	-3.902E-03	-2.993E-09	1.853E-03	1.265E-09	3.419E-04	6.013E-08	4.711E-02	1.810E-07	1.475E-03
q_9	-1.605E-14	-3.950E-08	-3.208E-14	2.023E-08	-3.875E-14	4.255E-10	1.586E-13	1.810E-07	4.997E-12	6.110E-08
q_{10}	-3.899E-10	-1.000E-03	-8.448E-10	5.383E-04	-1.653E-09	-2.054E-05	5.077E-10	1.475E-03	6.110E-08	3.237E-03

m_2	q_1	q_2	q_3	q_4	q_5	q_6	q_7	q_8	q_9	q_{10}
q_1	2.451E-11	1.034E-07	-1.140E-13	8.861E-08	-9.002E-13	-2.474E-08	-1.520E-12	-3.567E-07	-4.510E-12	-1.383E-07
q_2	1.034E-07	1.116E+02	3.996E-06	-1.695E+00	-2.224E-06	-7.796E-02	-5.277E-06	-1.341E+00	-1.757E-05	-5.495E-01
q_3	-1.140E-13	3.996E-06	8.210E-11	-3.483E-05	8.456E-13	-4.126E-08	-4.153E-12	-1.281E-06	-1.785E-11	-5.760E-07
q_4	8.861E-08	-1.695E+00	-3.483E-05	3.415E+01	-1.435E-06	1.749E-02	2.439E-06	8.229E-01	1.173E-05	3.821E-01
q_5	-9.002E-13	-2.224E-06	8.456E-13	-1.435E-06	7.563E-10	5.178E-06	9.232E-11	2.216E-06	-3.162E-11	-1.741E-06
q_6	-2.474E-08	-7.796E-02	-4.126E-08	1.749E-02	5.178E-06	4.311E-01	9.666E-06	3.393E-01	4.483E-07	-2.691E-02
q_7	-1.520E-12	-5.277E-06	-4.153E-12	2.439E-06	9.232E-11	9.666E-06	1.310E-09	6.087E-05	1.674E-10	1.863E-07
q_8	-3.567E-07	-1.341E+00	-1.281E-06	8.229E-01	2.216E-06	3.393E-01	6.087E-05	5.201E+01	2.125E-04	1.731E+00
q_9	-4.510E-12	-1.757E-05	-1.785E-11	1.173E-05	-3.162E-11	4.483E-07	1.674E-10	2.125E-04	6.328E-09	8.070E-05
q_{10}	-1.383E-07	-5.495E-01	-5.760E-07	3.821E-01	-1.741E-06	-2.691E-02	1.863E-07	1.731E+00	8.070E-05	4.571E+00

m_4	q_1	q_2	q_3	q_4	q_5	q_6	q_7	q_8	q_9	q_{10}
q_1	2.414E-07	7.491E-01	8.061E-07	-5.388E-01	3.150E-06	7.624E-02	4.124E-06	7.335E-01	6.421E-06	1.075E-01
q_2	7.491E-01	6.947E+06	3.605E+00	-2.368E+06	1.330E+01	3.212E+05	1.736E+01	3.085E+06	2.702E+01	4.533E+05
q_3	8.061E-07	3.605E+00	1.148E-05	-6.078E+00	1.531E-05	3.635E-01	1.949E-05	3.435E+00	2.988E-05	4.951E-01
q_4	-5.388E-01	-2.368E+06	-6.078E+00	5.505E+06	-1.051E+01	-2.473E+05	-1.321E+01	-2.319E+06	-2.012E+01	-3.318E+05
q_5	3.150E-06	1.330E+01	1.531E-05	-1.051E+01	3.951E-04	4.332E+00	1.468E-04	1.938E+01	1.509E-04	2.270E+00
q_6	7.624E-02	3.212E+05	3.635E-01	-2.473E+05	4.332E+00	3.104E+05	9.254E+00	7.513E+05	5.046E+00	7.246E+04
q_7	4.124E-06	1.736E+01	1.949E-05	-1.321E+01	1.468E-04	9.254E+00	1.211E-03	8.703E+01	4.580E-04	6.215E+00
q_8	7.335E-01	3.085E+06	3.435E+00	-2.319E+06	1.938E+01	7.513E+05	8.703E+01	6.869E+07	3.526E+02	3.942E+06
q_9	6.421E-06	2.702E+01	2.988E-05	-2.012E+01	1.509E-04	5.046E+00	4.580E-04	3.526E+02	1.084E-02	1.597E+02
q_{10}	1.075E-01	4.533E+05	4.951E-01	-3.318E+05	2.270E+00	7.246E+04	6.215E+00	3.942E+06	1.597E+02	9.646E+06

Table 4. Modal stress shapes (Element ID = 1678) [*MPa*] – test case no. 1

mode	1	2	3	4	5	6	7	8	9	10
σ_x	-4.9808	-2339.220	-44.3548	2380.730	270.174	-1674.570	229.266	10103.100	-410.759	-5064.990
σ_y	-2.1009	-291.873	-18.6471	305.261	114.040	-241.575	97.3701	1244.090	-173.384	-694.206
σ_z	0.0	0.0	0.0	0.0	0.0	0.0	0.0	0.0	0.0	0.0
τ_{xy}	-7.3344	-203.777	-65.0285	212.596	398.237	-166.705	340.718	861.386	-605.519	-475.090
τ_{xz}	0.0	0.0	0.0	0.0	0.0	0.0	0.0	0.0	0.0	0.0
τ_{yz}	0.0	0.0	0.0	0.0	0.0	0.0	0.0	0.0	0.0	0.0

Table 5. Computation times comparison – test case no. 1

Procedure type	**Computational Time** [*s*]
Reference Procedure (by *Dirlik*)	196
Proposed Procedure (by *Dirlik*)	0.9
Proposed Procedure (by *Bands*)	0.2

Table 6. Spectral moments and damage for some FE model elements – test case no. 1

Element ID	m_0 [MPa^2]	m_1 [$MPa^2 \cdot Hz$]	m_2 [$MPa^2 \cdot Hz^2$]	m_4 [$MPa^2 \cdot Hz^4$]	*D* (by *Dirlik*) [*no units*]	*D* (by *Bands*) [*no units*]
3224	$1.098 \cdot 10^4$	$3.853 \cdot 10^6$	$2.661 \cdot 10^9$	$2.872 \cdot 10^{15}$	$1.778 \cdot 10^{-3}$	$1.515 \cdot 10^{-3}$
3277	$1.102 \cdot 10^4$	$3.771 \cdot 10^6$	$2.547 \cdot 10^9$	$2.743 \cdot 10^{15}$	$1.789 \cdot 10^{-3}$	$1.513 \cdot 10^{-3}$
3360	$1.103 \cdot 10^4$	$3.774 \cdot 10^6$	$2.549 \cdot 10^9$	$2.745 \cdot 10^{15}$	$1.796 \cdot 10^{-3}$	$1.519 \cdot 10^{-3}$
3297	$1.219 \cdot 10^4$	$4.183 \cdot 10^6$	$2.833 \cdot 10^9$	$3.053 \cdot 10^{15}$	$2.963 \cdot 10^{-3}$	$2.507 \cdot 10^{-3}$
3339	$1.220 \cdot 10^4$	$4.186 \cdot 10^6$	$2.835 \cdot 10^9$	$3.055 \cdot 10^{15}$	$2.973 \cdot 10^{-3}$	$2.516 \cdot 10^{-3}$
3318	$1.262 \cdot 10^4$	$4.337 \cdot 10^6$	$2.940 \cdot 10^9$	$3.169 \cdot 10^{15}$	$3.532 \cdot 10^{-3}$	$2.990 \cdot 10^{-3}$
3223	$1.453 \cdot 10^4$	$5.178 \cdot 10^6$	$3.624 \cdot 10^9$	$3.938 \cdot 10^{15}$	$7.284 \cdot 10^{-3}$	$6.225 \cdot 10^{-3}$
3169	$1.515 \cdot 10^4$	$5.400 \cdot 10^6$	$3.780 \cdot 10^9$	$4.107 \cdot 10^{15}$	$8.984 \cdot 10^{-3}$	$7.679 \cdot 10^{-3}$
3186	$2.197 \cdot 10^4$	$7.885 \cdot 10^6$	$5.551 \cdot 10^9$	$6.049 \cdot 10^{15}$	$5.779 \cdot 10^{-2}$	$4.947 \cdot 10^{-2}$
1678	$2.219 \cdot 10^4$	$7.968 \cdot 10^6$	$5.612 \cdot 10^9$	$6.116 \cdot 10^{15}$	$6.082 \cdot 10^{-2}$	$5.207 \cdot 10^{-2}$

Table 7. Spectral moments of equivalent stress PSD function (Element ID = 67357) – test case no. 2

Procedure type	m_0 [MPa^2]	m_1 [$MPa^2 \cdot Hz$]	m_2 [$MPa^2 \cdot Hz^2$]	m_4 [$MPa^2 \cdot Hz^4$]
Reference Procedure	$8.672 \cdot 10^3$	$3.747 \cdot 10^4$	$1.680 \cdot 10^5$	$1.141 \cdot 10^7$
Proposed Procedure	$8.672 \cdot 10^3$	$3.747 \cdot 10^4$	$1.680 \cdot 10^5$	$1.141 \cdot 10^7$

Table 8. Spectral moments of PSD matrix of *Lagrangian* coordinates –test case no. 2

m_0	q_1	q_2	q_3	q_4	q_5	q_6	q_7	q_8	q_9	q_{10}	q_{11}	q_{12}	q_{13}	q_{14}	q_{15}
q_1	4.060E+01	7.116E-08	-4.331E-02	2.788E-06	4.586E-09	-1.078E-05	1.989E-08	1.152E-08	5.470E-04	-6.421E-09	8.059E-08	5.061E-07	1.321E-03	4.349E-08	8.627E-10
q_2	7.116E-08	1.208E-13	-3.690E-08	8.261E-14	1.389E-16	-3.309E-13	6.147E-16	4.486E-16	2.188E-11	-2.825E-16	3.864E-15	2.430E-14	6.353E-11	2.119E-15	4.336E-17
q_3	-4.331E-02	-3.690E-08	4.598E-02	-1.005E-07	-1.584E-10	3.719E-07	-6.859E-10	-4.379E-10	-2.114E-05	2.639E-10	-3.517E-09	-2.211E-08	-5.779E-05	-1.920E-09	-3.900E-11
q_4	2.788E-06	8.261E-14	-1.005E-07	1.511E-10	1.627E-13	-3.273E-10	5.603E-13	1.248E-13	5.733E-09	-6.283E-14	7.766E-13	4.877E-12	1.273E-08	4.196E-13	8.379E-15
q_5	4.586E-09	1.389E-16	-1.584E-10	1.627E-13	3.959E-16	-8.978E-13	1.592E-15	2.422E-16	1.087E-11	-1.133E-16	1.376E-15	8.640E-15	2.256E-11	7.424E-16	1.480E-17
q_6	-1.078E-05	-3.309E-13	3.719E-07	-3.273E-10	-8.978E-13	2.172E-09	-3.967E-12	-5.982E-13	-2.661E-08	2.727E-13	-3.293E-12	-2.068E-11	-5.398E-08	-1.776E-12	-3.538E-14
q_7	1.989E-08	6.147E-16	-6.859E-10	5.603E-13	1.592E-15	-3.967E-12	7.360E-15	1.132E-15	5.013E-11	-5.090E-16	6.127E-15	3.847E-14	1.004E-10	3.303E-15	6.579E-17
q_8	1.152E-08	4.486E-16	-4.379E-10	1.248E-13	2.422E-16	-5.982E-13	1.132E-15	2.188E-15	9.437E-11	-4.938E-16	4.552E-15	2.853E-14	7.431E-11	2.407E-15	4.691E-17
q_9	5.470E-04	2.188E-11	-2.114E-05	5.733E-09	1.087E-11	-2.661E-08	5.013E-11	9.437E-11	4.851E-06	-2.705E-11	2.261E-10	1.416E-09	3.685E-06	1.187E-10	2.296E-12
q_{10}	-6.421E-09	-2.825E-16	2.639E-10	-6.283E-14	-1.133E-16	2.727E-13	-5.090E-16	-4.938E-16	-2.705E-11	6.229E-16	-3.600E-15	-2.240E-14	-5.786E-11	-1.769E-15	-3.173E-17
q_{11}	8.059E-08	3.864E-15	-3.517E-09	7.766E-13	1.376E-15	-3.293E-12	6.127E-15	4.552E-15	2.261E-10	-3.600E-15	9.174E-14	5.755E-13	1.498E-09	4.536E-14	6.288E-16
q_{12}	5.061E-07	2.430E-14	-2.211E-08	4.877E-12	8.640E-15	-2.068E-11	3.847E-14	2.853E-14	1.416E-09	-2.240E-14	5.755E-13	3.615E-12	9.426E-09	2.883E-13	4.004E-15
q_{13}	1.321E-03	6.353E-11	-5.779E-05	1.273E-08	2.256E-11	-5.398E-08	1.004E-10	7.431E-11	3.685E-06	-5.786E-11	1.498E-09	9.426E-09	2.462E-05	7.628E-10	1.063E-11
q_{14}	4.349E-08	2.119E-15	-1.920E-09	4.196E-13	7.424E-16	-1.776E-12	3.303E-15	2.407E-15	1.187E-10	-1.769E-15	4.536E-14	2.883E-13	7.628E-10	2.653E-14	4.057E-16
q_{15}	8.627E-10	4.336E-17	-3.900E-11	8.379E-15	1.480E-17	-3.538E-14	6.579E-17	4.691E-17	2.296E-12	-3.173E-17	6.288E-16	4.004E-15	1.063E-11	4.057E-16	1.049E-17

m_1	q_1	q_2	q_3	q_4	q_5	q_6	q_7	q_8	q_9	q_{10}	q_{11}	q_{12}	q_{13}	q_{14}	q_{15}
q_1	1.755E+02	6.271E-07	-4.130E-01	3.605E-05	6.017E-08	-1.419E-04	2.621E-07	1.549E-07	7.357E-03	-8.614E-08	1.067E-06	6.696E-06	1.747E-02	5.728E-07	1.121E-08
q_2	6.271E-07	1.775E-12	-5.526E-07	-3.294E-12	-5.725E-15	1.357E-11	-2.511E-14	-1.450E-14	-6.826E-10	7.621E-15	-8.679E-14	-5.437E-13	-1.416E-09	-4.546E-14	-8.331E-16
q_3	-4.130E-01	-5.526E-07	7.565E-01	1.339E-06	2.598E-09	-6.258E-06	1.166E-08	7.131E-09	3.352E-04	-3.677E-09	3.982E-08	2.491E-07	6.476E-04	2.048E-08	3.559E-10
q_4	3.605E-05	-3.294E-12	1.339E-06	4.322E-09	4.533E-12	-8.881E-09	1.497E-11	1.890E-12	8.247E-08	-8.023E-13	1.007E-11	6.334E-11	1.657E-07	5.561E-12	1.185E-13
q_5	6.017E-08	-5.725E-15	2.598E-09	4.533E-12	1.227E-14	-2.798E-11	4.956E-14	4.584E-15	1.927E-10	-1.702E-15	2.041E-14	1.283E-13	3.356E-10	1.122E-14	2.376E-16
q_6	-1.419E-04	1.357E-11	-6.258E-06	-8.881E-09	-2.798E-11	6.868E-08	-1.259E-10	-1.200E-11	-4.985E-07	4.269E-12	-5.048E-11	-3.174E-10	-8.297E-07	-2.771E-11	-5.859E-13
q_7	2.621E-07	-2.511E-14	1.166E-08	1.497E-11	4.956E-14	-1.259E-10	2.350E-13	2.338E-14	9.651E-10	-8.130E-15	9.544E-14	5.999E-13	1.568E-09	5.235E-14	1.106E-15
q_8	1.549E-07	-1.450E-14	7.131E-09	1.890E-12	4.584E-15	-1.200E-11	2.338E-14	9.105E-14	3.920E-09	-1.563E-14	1.140E-13	7.133E-13	1.856E-09	5.985E-14	1.200E-15
q_9	7.357E-03	-6.826E-10	3.352E-04	8.247E-08	1.927E-10	-4.985E-07	9.651E-10	3.920E-09	2.090E-04	-9.590E-10	6.103E-09	3.816E-08	9.913E-05	3.164E-09	6.243E-11
q_{10}	-8.614E-08	7.621E-15	-3.677E-09	-8.023E-13	-1.702E-15	4.269E-12	-8.130E-15	-1.563E-14	-9.590E-10	3.112E-14	-1.420E-13	-8.793E-13	-2.259E-09	-6.633E-14	-1.146E-15
q_{11}	1.067E-06	-8.679E-14	3.982E-08	1.007E-11	2.041E-14	-5.048E-11	9.544E-14	1.140E-13	6.103E-09	-1.420E-13	5.561E-12	3.495E-11	9.114E-08	2.750E-12	3.527E-14
q_{12}	6.696E-06	-5.437E-13	2.491E-07	6.334E-11	1.283E-13	-3.174E-10	5.999E-13	7.133E-13	3.816E-08	-8.793E-13	3.495E-11	2.200E-10	5.748E-07	1.758E-11	2.265E-13
q_{13}	1.747E-02	-1.416E-09	6.476E-04	1.657E-07	3.356E-10	-8.297E-07	1.568E-09	1.856E-09	9.913E-05	-2.259E-09	9.114E-08	5.748E-07	1.505E-03	4.680E-08	6.073E-10
q_{14}	5.728E-07	-4.546E-14	2.048E-08	5.561E-12	1.122E-14	-2.771E-11	5.235E-14	5.985E-14	3.164E-09	-6.633E-14	2.750E-12	1.758E-11	4.680E-08	1.686E-12	2.514E-14
q_{15}	1.121E-08	-8.331E-16	3.559E-10	1.185E-13	2.376E-16	-5.859E-13	1.106E-15	1.200E-15	6.243E-11	-1.146E-15	3.527E-14	2.265E-13	6.073E-10	2.514E-14	7.431E-16

m_2	q_1	q_2	q_3	q_4	q_5	q_6	q_7	q_8	q_9	q_{10}	q_{11}	q_{12}	q_{13}	q_{14}	q_{15}
q_1	7.850E+02	2.756E-06	-2.321E+00	4.240E-04	7.301E-07	-1.733E-03	3.211E-06	1.964E-06	9.299E-02	-1.045E-06	1.107E-05	6.916E-05	1.795E-01	5.575E-06	8.863E-08
q_2	2.756E-06	2.714E-11	-8.963E-06	-9.292E-11	-1.668E-13	3.986E-10	-7.406E-13	-4.581E-13	-2.158E-08	2.328E-13	-2.145E-12	-1.334E-11	-3.441E-08	-1.009E-12	-1.197E-14
q_3	-2.321E+00	-8.963E-06	1.294E+01	4.956E-05	9.542E-08	-2.305E-04	4.302E-07	2.786E-07	1.312E-02	-1.391E-07	1.170E-06	7.251E-06	1.863E-02	5.219E-07	4.379E-09
q_4	4.240E-04	-9.292E-11	4.956E-05	1.334E-07	1.429E-10	-2.793E-07	4.697E-10	4.531E-11	1.912E-06	-1.864E-11	3.217E-10	2.040E-09	5.385E-06	1.956E-10	5.141E-12
q_5	7.301E-07	-1.668E-13	9.542E-08	1.429E-10	4.153E-13	-9.563E-10	1.700E-12	1.369E-13	5.592E-09	-4.838E-14	7.444E-13	4.711E-12	1.242E-08	4.443E-13	1.132E-14
q_6	-1.733E-03	3.986E-10	-2.305E-04	-2.793E-07	-9.563E-10	2.378E-06	-4.383E-09	-3.762E-10	-1.520E-05	1.270E-10	-1.900E-09	-1.202E-08	-3.167E-05	-1.129E-09	-2.857E-11
q_7	3.211E-06	-7.406E-13	4.302E-07	4.697E-10	1.700E-12	-4.383E-09	8.231E-12	7.499E-13	3.013E-08	-2.472E-13	3.648E-12	2.307E-11	6.077E-08	2.163E-12	5.454E-14
q_8	1.964E-06	-4.581E-13	2.786E-07	4.531E-11	1.369E-13	-3.762E-10	7.499E-13	4.389E-12	1.923E-07	-7.828E-13	6.389E-12	4.015E-11	1.049E-07	3.530E-12	8.010E-14
q_9	9.299E-02	-2.158E-08	1.312E-02	1.912E-06	5.592E-09	-1.520E-05	3.013E-08	1.923E-07	1.053E-02	-5.047E-08	3.577E-07	2.245E-06	5.857E-03	1.945E-07	4.323E-09
q_{10}	-1.045E-06	2.328E-13	-1.391E-07	-1.864E-11	-4.838E-14	1.270E-10	-2.472E-13	-7.828E-13	-5.047E-08	1.896E-12	-9.764E-12	-6.063E-11	-1.563E-07	-4.750E-12	-9.102E-14
q_{11}	1.107E-05	-2.145E-12	1.170E-06	3.217E-10	7.444E-13	-1.900E-09	3.648E-12	6.389E-12	3.577E-07	-9.764E-12	4.353E-10	2.742E-09	7.172E-06	2.223E-10	3.127E-12
q_{12}	6.916E-05	-1.334E-11	7.251E-06	2.040E-09	4.711E-12	-1.202E-08	2.307E-11	4.015E-11	2.245E-06	-6.063E-11	2.742E-09	1.730E-08	4.534E-05	1.424E-09	2.011E-11
q_{13}	1.795E-01	-3.441E-08	1.863E-02	5.385E-06	1.242E-08	-3.167E-05	6.077E-08	1.049E-07	5.857E-03	-1.563E-07	7.172E-06	4.534E-05	1.191E-01	3.800E-06	5.399E-08
q_{14}	5.575E-06	-1.009E-12	5.219E-07	1.956E-10	4.443E-13	-1.129E-09	2.163E-12	3.530E-12	1.945E-07	-4.750E-12	2.223E-10	1.424E-09	3.800E-06	1.399E-10	2.263E-12
q_{15}	8.863E-08	-1.197E-14	4.379E-09	5.141E-12	1.132E-14	-2.857E-11	5.454E-14	8.010E-14	4.323E-09	-9.102E-14	3.127E-12	2.011E-11	5.399E-08	2.263E-12	6.978E-14

m_4	q_1	q_2	q_3	q_4	q_5	q_6	q_7	q_8	q_9	q_{10}	q_{11}	q_{12}	q_{13}	q_{14}	q_{15}
q_1	3.894E+04	-7.814E-03	5.546E+03	-9.194E-01	-1.835E-03	4.532E+00	-8.564E-03	-9.786E-03	-5.099E+02	8.895E-03	-1.855E-01	-1.176E+00	-3.106E+03	-1.125E-01	-2.872E-03
q_2	-7.814E-03	9.032E-09	-4.329E-03	3.183E-07	6.348E-10	-1.568E-06	2.963E-09	3.423E-09	1.786E-04	-3.135E-09	6.576E-08	4.170E-07	1.101E-03	3.994E-08	1.021E-09
q_3	5.546E+03	-4.329E-03	5.234E+03	-2.393E-01	-4.736E-04	1.168E+00	-2.207E-03	-2.533E-03	-1.322E+02	2.319E-03	-4.865E-02	-3.085E-01	-8.147E+02	-2.955E-02	-7.558E-04
q_4	-9.194E-01	3.183E-07	-2.393E-01	1.894E-04	2.663E-07	-5.820E-04	1.039E-06	6.297E-07	3.216E-02	-5.366E-07	1.099E-05	6.969E-05	1.840E-01	6.658E-06	1.696E-07
q_5	-1.835E-03	6.348E-10	-4.736E-04	2.663E-07	7.265E-10	-1.737E-06	3.171E-09	1.361E-09	6.850E-05	-1.110E-09	2.250E-08	1.426E-07	3.765E-04	1.361E-08	3.463E-10
q_6	4.532E+00	-1.568E-06	1.168E+00	-5.820E-04	-1.737E-06	4.383E-03	-8.205E-06	-3.447E-06	-1.726E-01	2.766E-06	-5.589E-05	-3.543E-04	-9.352E-01	-3.381E-05	-8.596E-07
q_7	-8.564E-03	2.963E-09	-2.207E-03	1.039E-06	3.171E-09	-8.205E-06	1.557E-08	6.603E-09	3.295E-04	-5.251E-09	1.059E-07	6.713E-07	1.772E-03	6.406E-08	1.628E-09
q_8	-9.786E-03	3.423E-09	-2.533E-03	6.297E-07	1.361E-09	-3.447E-06	6.603E-09	1.698E-08	8.136E-04	-7.770E-09	1.327E-07	8.404E-07	2.216E-03	7.934E-08	1.987E-09
q_9	-5.099E+02	1.786E-04	-1.322E+02	3.216E-02	6.850E-05	-1.726E-01	3.295E-04	8.136E-04	4.486E+01	-4.409E-04	7.048E-03	4.461E-02	1.175E+02	4.196E-03	1.046E-04
q_{10}	8.895E-03	-3.135E-09	2.319E-03	-5.366E-07	-1.110E-09	2.766E-06	-5.251E-09	-7.770E-09	-4.409E-04	1.208E-08	-1.423E-07	-8.965E-07	-2.351E-03	-8.123E-08	-1.935E-09
q_{11}	-1.855E-01	6.576E-08	-4.865E-02	1.099E-05	2.250E-08	-5.589E-05	1.059E-07	1.327E-07	7.048E-03	-1.423E-07	4.469E-06	2.828E-05	7.442E-02	2.513E-06	4.955E-08
q_{12}	-1.176E+00	4.170E-07	-3.085E-01	6.969E-05	1.426E-07	-3.543E-04	6.713E-07	8.404E-07	4.461E-02	-8.965E-07	2.828E-05	1.791E-04	4.719E-01	1.605E-05	3.164E-07
q_{13}	-3.106E+03	1.101E-03	-8.147E+02	1.840E-01	3.765E-04	-9.352E-01	1.772E-03	2.216E-03	1.175E+02	-2.351E-03	7.442E-02	4.719E-01	1.245E+03	4.270E-02	8.425E-04

q_{14}	-1.125E-01	3.994E-08	-2.955E-02	6.658E-06	1.361E-08	-3.381E-05	6.406E-08	7.934E-08	4.196E-03	-8.123E-08	2.513E-06	1.605E-05	4.270E-02	1.587E-06	3.299E-08
q_{15}	-2.872E-03	1.021E-09	-7.558E-04	1.696E-07	3.463E-10	-8.596E-07	1.628E-09	1.987E-09	1.046E-04	-1.935E-09	4.955E-08	3.164E-07	8.425E-04	3.299E-08	9.602E-10

Table 9. Modal stress shapes (Element ID = 67357) [*MPa*] – test case no. 2

mode	1	2	3	4	5	6	7	8	9	10	11	12	13	14	15
σ_x	-14.6614	9.1214	-7.8629	62.3638	17.7904	18.0816	-4.8335	53.7383	79.1259	142.433	51.1746	-75.6424	1.8068	-183.105	-105.183
σ_y	-4.4488	0.258	0.2486	18.2249	-0.1014	-0.0077	-2.8973	11.8317	24.3716	33.4705	11.5092	-23.2718	-5.1998	-46.5001	-26.5195
σ_z	0.0	0.0	0.0	0.0	0.0	0.0	0.0	0.0	0.0	0.0	0.0	0.0	0.0	0.0	0.0
τ_{xy}	-3.8405	0.4777	0.0194	15.7716	0.5823	0.3482	-1.1262	14.6129	21.3066	34.6082	12.4617	-23.8022	-4.6666	-40.6511	-25.7943
τ_{xz}	0.0	0.0	0.0	0.0	0.0	0.0	0.0	0.0	0.0	0.0	0.0	0.0	0.0	0.0	0.0
τ_{yz}	0.0	0.0	0.0	0.0	0.0	0.0	0.0	0.0	0.0	0.0	0.0	0.0	0.0	0.0	0.0

Table 10. Computation times comparison – test case no. 2

Procedure type	**Computational Time** [*s*]
Reference Procedure (by *Dirlik*)	1594
Proposed Procedure (by *Dirlik*)	13.33
Proposed Procedure (by *Bands*)	1.7

Table 11. Spectral moments and damage for some FE model elements – test case no. 2

Element ID	m_0 [MPa^2]	m_1 [$MPa^2 \cdot Hz$]	m_2 [$MPa^2 \cdot Hz^2$]	m_4 [$MPa^2 \cdot Hz^4$]	*D* (by *Dirlik*) [*no units*]	*D* (by *Bands*) [*no units*]
71981	$4.424 \cdot 10^3$	$1.927 \cdot 10^4$	$8.845 \cdot 10^4$	$9.707 \cdot 10^6$	$5.370 \cdot 10^{-6}$	$1.844 \cdot 10^{-6}$
68136	$4.616 \cdot 10^3$	$2.010 \cdot 10^4$	$9.207 \cdot 10^4$	$9.080 \cdot 10^6$	$6.349 \cdot 10^{-6}$	$2.375 \cdot 10^{-6}$
69408	$5.267 \cdot 10^3$	$2.404 \cdot 10^4$	$1.262 \cdot 10^5$	$1.365 \cdot 10^7$	$7.930 \cdot 10^{-6}$	$5.359 \cdot 10^{-6}$
71909	$5.289 \cdot 10^3$	$2.285 \cdot 10^4$	$1.024 \cdot 10^5$	$6.697 \cdot 10^6$	$8.165 \cdot 10^{-6}$	$5.311 \cdot 10^{-6}$
67358	$5.331 \cdot 10^3$	$2.303 \cdot 10^4$	$1.032 \cdot 10^5$	$6.754 \cdot 10^6$	$8.557 \cdot 10^{-6}$	$5.570 \cdot 10^{-6}$
69433	$5.151 \cdot 10^3$	$2.318 \cdot 10^4$	$1.180 \cdot 10^5$	$2.483 \cdot 10^7$	$8.688 \cdot 10^{-6}$	$4.652 \cdot 10^{-6}$
71983	$5.417 \cdot 10^3$	$2.362 \cdot 10^4$	$1.088 \cdot 10^5$	$1.355 \cdot 10^7$	$1.869 \cdot 10^{-5}$	$6.164 \cdot 10^{-6}$
68155	$5.634 \cdot 10^3$	$2.455 \cdot 10^4$	$1.128 \cdot 10^5$	$1.255 \cdot 10^7$	$2.274 \cdot 10^{-5}$	$7.786 \cdot 10^{-6}$
71905	$8.589 \cdot 10^3$	$3.711 \cdot 10^4$	$1.664 \cdot 10^5$	$1.142 \cdot 10^7$	$1.602 \cdot 10^{-4}$	$9.523 \cdot 10^{-5}$
67357	$8.672 \cdot 10^3$	$3.747 \cdot 10^4$	$1.680 \cdot 10^5$	$1.141 \cdot 10^7$	$1.660 \cdot 10^{-4}$	$1.008 \cdot 10^{-4}$